

G α 12 Inhibits α 2 β 1 Integrin–mediated Madin-Darby Canine Kidney Cell Attachment and Migration on Collagen-I and Blocks Tubulogenesis

Tianqing Kong,* Daosong Xu,[†] Wanfeng Yu,* Ayumi Takakura,* Ilene Boucher,* Mei Tran,* Jordan A. Kreidberg,[‡] Jagesh Shah,* Jing Zhou,* and Bradley M. Denker*

*Renal Division, Brigham and Women's Hospital, Harvard Institutes of Medicine, Boston, MA 02115; [†]Dana Farber Cancer Institute, Boston, MA 02115; and [‡]Children's Hospital, Boston, MA 02115

Submitted March 18, 2009; Revised August 19, 2009; Accepted September 15, 2009
Monitoring Editor: Asma Nusrat

Regulation of epithelial cell attachment and migration are essential for normal development and maintenance of numerous tissues. G proteins and integrins are critical signaling proteins regulating these processes, yet in polarized cells little is known about the interaction of these pathways. Herein, we demonstrate that G α 12 inhibits interaction of MDCK cells with collagen-I, the major ligand for α 2 β 1 integrin. Activating G α 12 (QL point mutation or stimulating endogenous G α 12 with thrombin) inhibited focal adhesions and lamellipodia formation and led to impaired cell migration. Consistent with G α 12-regulated attachment to collagen-I, G α 12-silenced MDCK cells revealed a more adherent phenotype. Inhibiting Rho kinase completely restored normal attachment in G α 12-activated cells, and there was partial recovery with inhibition of Src and protein phosphatase pathways. G α 12 activation led to decreased phosphorylation of focal adhesion kinase and paxillin with displacement of α 2 integrin from the focal adhesion protein complex. Using the MDCK cell 3D-tubulogenesis assay, activated G α 12 inhibited tubulogenesis and led to the formation of cyst-like structures. Furthermore, G α 12-silenced MDCK cells were resistant to thrombin-stimulated cyst development. Taken together, these studies provide direct evidence for G α 12–integrin regulation of epithelial cell spreading and migration necessary for normal tubulogenesis.

INTRODUCTION

The regulation of cell interactions with the extracellular matrix is a critical component of cell migration, and these processes are fundamental to normal tissue development, recovery from injury, and malignant transformation. Many signaling pathways have been implicated in the complex and highly coordinated sequence of events needed for cells to migrate, and these include heterotrimeric G proteins, receptor tyrosine kinases, monomeric G proteins (especially Rho), and integrins. However, the link between G protein signaling and integrins regulating cell migration has only been partially explored in hematopoietic cells, and very little is known about these pathways in other cell types, especially epithelia. Defining these pathways in epithelial cells is critical for understanding the metastatic potential of epithelial cell cancers, renal development, and other disorders such as autosomal dominant polycystic kidney disease (ADPKD) where cell attachment and migration contribute to the disease process (Joly *et al.*, 2003; Battini *et al.*, 2006; Boca *et al.*, 2007).

The cell–matrix interaction involves an initial binding step that is then followed by cell spreading and the formation of focal adhesions and stress fibers (reviewed in Mitra *et al.*, 2005). The interaction of the cell with the matrix is mediated by integrins, a large family of heterodimeric (α and β subunits) single transmembrane glycoproteins. There are at least 18 α and 8 β subunits that have been identified, and they assemble into 24 distinct integrins (reviewed in Hynes, 2002.) Many integrins can bind more than one ligand, but α 1 β 1 and α 2 β 1 are predominantly collagen receptors, whereas α 4 β 1 and α 6 β 1 recognize mainly laminins. These integrins are present in most types of epithelium, and they are localized to the apical and lateral membranes in addition to the basal surface. Heterotrimeric G proteins (four major families named for the G α subunit (G α s, G α i/o, G α q, and G α 12/13) are ubiquitously expressed and signal through seven transmembrane receptors. Signaling through G proteins involves GTP binding to G α , disassociation of G α from G β γ and interaction with downstream effectors until the system is reset by the hydrolysis of GTP to GDP on G α . Integrins and G proteins converge on common signaling pathways including Rho and nonreceptor tyrosine kinases such as Src. In hematopoietic cells and fibroblasts, some details of G protein regulation of migration through integrins have started to emerge. In splenic B-cells, lysophosphatidic acid regulated integrin-mediated adhesion through G α i and G α 12/13 pathways (Rieken *et al.*, 2006), and in migrating leukocytes, the leading edge was dependent on G α i-mediated production of 3'-phosphoinositol lipids and activated Rac. The trailing edge used G α 12/13 regulation of

This article was published online ahead of print in *MBC in Press* (<http://www.molbiolcell.org/cgi/doi/10.1091/mbc.E09-03-0220>) on September 23, 2009.

Address correspondence to: Bradley M. Denker (bdenker@rics.bwh.harvard.edu).

Abbreviations used: dox; doxycycline; ADPKD, autosomal dominant polycystic kidney disease.

Rho, and both systems coordinated differential regulation of the actin cytoskeleton in the presence of a chemoattractant (Xu *et al.*, 2003). In platelets, integrin-mediated aggregation was stimulated with thrombin, ADP, epinephrine, thromboxane, and other agonists that utilize numerous G protein-coupled pathways. Costimulation of G α 12/13 and G α i pathways (with thromboxane A₂ and ADP) led to irreversible integrin (α IIb β 3)-mediated aggregation (Dorsam *et al.*, 2002; Nieswandt *et al.*, 2002). In fibroblasts, G α 12/13 were required for directed cell migration in wound healing assays, and cells lacking G α 12/13 were unable to localize active Rho or its effector mDia at the wound edge (Goulimari *et al.*, 2005).

G α 12/13 have major cellular roles that include regulating cell growth, transformation, and polarity (reviewed in Kelly *et al.*, 2007). G α 12/13 also have unique functions regulating actin stress-fiber formation (Buhl *et al.*, 1995; through direct activation of Rho; Kozasa *et al.*, 1998) and of cell-cell adhesion through interactions with adherens junction protein, E-cadherin, and tight junction protein, ZO-1 (Meigs *et al.*, 2002; Meyer *et al.*, 2002). Therefore, G α 12/13 are well situated to modulate signaling events in epithelial cell migration, yet to date, little is known about these mechanisms. In addition, elevated G α 12/13 protein levels were described in prostate and breast cancer, and this was associated with increased invasion and metastasis but not proliferation (Kelly *et al.*, 2006a,b). In the studies described here, we identify novel and specific regulation of epithelial cell attachment and migration through G α 12 and α 2 β 1 integrin when grown on collagen-I. We have identified the major signaling pathways and mechanisms leading to loss of cell attachment and extend these observations in to a model of epithelial morphogenesis.

MATERIALS AND METHODS

Cell Culture and Materials

The development and characterization of Tet-off inducible G α 12 and QL α 12 Madin-Darby canine kidney (MDCK) cell lines have been previously described (Meyer *et al.*, 2002). Plasticware and tissue culture supplies were from BD Bioscience (San Jose, CA). Chemicals were from Sigma (St. Louis, MO) unless otherwise indicated. G α 12 antibody was from Santa Cruz Biotechnology (Santa Cruz, CA). Src pTyr-418 was from Invitrogen (Carlsbad, CA), and total c-Src was from Santa Cruz. α 2 (5E8), α 3 (A3-IIF5) and β 1 (TS2/16) integrin antibodies were kindly provided by Dr. Martin Hemler (Harvard University; Zylstra *et al.*, 1986; Kolesnikova *et al.*, 2001). Collagen-IV was from BD Biosciences, and laminin-1 was from R&D Systems (Minneapolis, MN). Laminin-5 was provided by Martin Hemler, and Matrigel (BD Biosciences), fibronectin, and vitronectin were used as described previously (Yang *et al.*, 2008). Collagen type-I rat tail was from BD Biosciences. PP2 [4-amino-5-(4-chlorophenyl)-7-(*t*-butyl)pyrazolo[3,4-d]pyrimidine, Src Inhibitor] and Y27632 (Rho-associated protein kinase inhibitor) were from Calbiochem. Sodium orthovanadate was from Sigma. The α 2 β 1 blocking antibody (mouse anti-human VLA-2) was from Chemicon (Temecula, CA; Wang and Frazier, 1998). Total focal adhesion kinase (FAK) antibody was from BD Biosciences. The phospho-FAK antibodies were included in a kit (Biosource, Camarillo, CA). An additional pFAK397 was from ECM Biosciences (Versailles, KY). Total Paxillin (H-114) was from Santa Cruz. Paxillin 118 was from Cell Signaling Technology (Beverly, MA).

Immunoprecipitation and Western Blot

G α 12- or QL α 12-expressing MDCK cells were cultured with or without (\pm) doxycycline (dox). Monolayers were scraped in lysis buffer (150 mM NaCl, 2.5 mM EDTA, 25 mM HEPES, pH 7.5, 1 mM PMSF, 1% Triton X-100, and protease inhibitors; Roche, Indianapolis, IN) and phosphatase inhibitor cocktail (Sigma) plus 1 mM NaVO₄ and 25 mM NaF, as needed for detection of phospho-proteins, frozen/thawed, triturated, and centrifuged. Immunoprecipitations of α 2 integrin were done with protein A-Sepharose or goat affinity-purified rat IgG beads (MP Biomedicals, Aurora, OH) overnight at 4°C. Beads were centrifuged and washed three times, and proteins were eluted in SDS-PAGE sample buffer (nonreducing). SDS-PAGE was followed by Western blot transfer as previously described (Meyer *et al.*, 2002). After blocking and washing, primary antibodies to FAK were added overnight followed by

incubation with secondary horseradish peroxidase-conjugated antibodies for 1 h. Signal was detected with SuperSignal West Pico horseradish peroxidase substrate system (Pierce, Rockford, IL) and autoradiography (Biomax MR; Eastman Kodak, Rochester, NY).

Cell Attachment Studies

Plasticware was precoated with laminin-1 (10 μ g/ml), laminin-5 (1:100), Matrigel (1:200), collagen-I (8.6 μ g/ml), fibronectin (10 μ g/ml), vitronectin (1:100), and collagen-IV (10 mg/ml). Bovine serum albumin (BSA; 10 mg/ml) was sterile-filtered, then heated to 85°C for 10 min, and cooled to room temperature (RT). One hundred microliters was added to a 96-well plate and incubated at 37°C for 30 min. MDCK cells were grown to 60–90% confluence under standard conditions, and washed twice with PBS, and Calcein Am (Invitrogen) stock (5 μ l, in 1 ml of DMEM (serum free) was added to the cells and incubated at 37°C for 30 min. Cells were washed twice with PBS, and detached cells were counted, gently centrifuged for 5 min, and resuspended at 2.5×10^5 /ml. One hundred microliters was added to each well of a 96-well plate and incubated at 37°C for 20–30 min. Each well was washed three times with PBS, and fluorescence measured using a CytoFluor 2300, fluorimeter (Millipore, Bedford, MA). Each condition was performed with $n = 4$, and the experiment was repeated at least three times. Agonists (2 U/ml thrombin and 100 μ M bradykinin) were added after cells were detached for 30 min and then were analyzed for adhesion to collagen-I.

FACS Analysis

G α 12- and QL α 12-MDCK cells \pm dox for 48 h were surface-labeled with antibodies to α 2 and β 1 integrin. Control antibody was mouse IgG (Sigma). Cells were grown to 90% confluence, washed once with PBS, and detached with detachment buffer. Cells were washed with PBS and filtered through a 40- μ m sieve, and 5×10^5 /ml cells were suspended in each well of a 96-well plate (flat bottom) with fluorescence-activated cell sorting (FACS) buffer (5% heat-inactivated goat serum, 1% BSA, and 0.1% NaN₃ in PBS) and kept on ice for 1 h. Cells were then incubated with specific antibodies (10 μ g/ml in FACS buffer) on ice for 1 h. Cells were washed three times in FACS buffer, centrifuged, and incubated with goat anti-mouse IgG-FITC (Biosource; 1:100 in FACS buffer) for 1 h. After washing with PBS, cells were resuspended and analyzed by FACS Calibur (BD Biosciences). Data were analyzed with FlowJo software (Free Star, Ashland, OR), and each antibody staining was done with three wells and repeated at least three times.

Cell Spreading

Plasticware was coated with Collagen-I (8.6 μ g/ml) at 37°C for 1 h. Plates were washed once with PBS and then blocked with BSA (10 mg/ml) for 30 min at 37°C. Cells were detached as described above but resuspended at 1×10^5 /ml, and 0.5 ml placed in each of the 24 wells. Cells were observed continuously for 20–40 min and then gently washed twice with PBS, fixed in paraformaldehyde (PFA; 4%), and stained with Giemsa (Sigma) (1:20 dilution in water for 30 min), washed three times with water, and then imaged.

Cell Invasion

Transwell filters (8- μ m pore size, 6.5-mm diameter; Corning, Corning, NY) were coated with collagen-I as described above. Cells, 5×10^4 in 100 μ l serum free medium, were placed in the apical chamber, and 600 μ l medium containing hepatocyte growth factor (HGF; 20 ng/ml; Sigma) was added to the bottom chamber. Cultures were incubated at 37°C overnight, washed twice with PBS, and then fixed with ice-cold methanol for 6 min. After air drying, cells were stained with Giemsa and the bottom surface of the filter photographed for cell migrating through the filter.

Scratch Wound Assay and Videomicroscopy

G α 12- and QL α 12-MDCK cells (\pm dox) were plated on a collagen-I coated 10-cm² plate. After reaching confluence, the surfaces were scratched with a 10- μ l extended length pipette tip and maintained in a humidified chamber. Each condition was imaged on a Nikon TE 2000E2 microscope (Melville, NY), captured to a COOLSNAP HQ cooled CCD (Photometrics, Tucson, AZ), and analyzed with IPLab software (Scanalytics, Fairfax, VA). Images were obtained every 10 min. Wound closure rate was calculated by measuring the area of the gap over time using Image J (1.38, Wayne Rasband, NIH, <http://rsb.info.nih.gov/ij/>). Tet-off MDCK cells were analyzed under identical conditions \pm thrombin (2 U/ml) added to the medium at the time of scratching ($t = 0$).

Immunofluorescence and Confocal Microscopy

G α 12- and QL α 12-MDCK cells were cultured at subconfluent density on collagen-I-coated culture slide chambers (Falcon plates; BD Labware, Bedford, MA) for 48 h \pm dox. Cultures were fixed with 3.7% PFA for 15 min, followed by ice-cold acetone for 10 min and two washes with PBS. Blocking was done for 1 h at RT with 1% BSA and 2% goat serum in PBS. Cultures were then washed three times with PBS followed by incubation with vinculin-FITC (mAb from Sigma, in 1% BSA in PBS, 1:50) for 1 h at RT. Cultures were

washed three times with PBS and mounted with DAPI-containing mounting (Vector Laboratories, Burlingame, CA). Images were obtained using a Zeiss Confocal LSM510 microscope (Thornwood, NY) and figures were assembled as described above. Phalloidin staining (1:200) was done for 30 min under identical cell culture conditions. $\alpha 2$ and $\beta 1$ integrin staining was performed using similar conditions and appropriate secondary antibodies.

RhoA Activation

Rho activation was determined using rhotekin-RBD (Rho-binding domain) beads according to the manufacturer's instructions (Cytoskeleton, Denver, CO). Briefly, subconfluent 10-cm² plates were placed in 1% serum for 8 h followed by 16 h in serum-free medium. Lysates were incubated with rhotekin beads at 4°C for 1 h. Beads were pelleted, washed, and eluted followed by Western blot for Rho A. Controls included incubating +dox lysates with GDP (1 mM, negative control) or GTP γ S (200 μ M, positive control) for 15 min and then analyzing with parallel samples from wild-type and QL α 12-MDCK cells \pm dox.

Inhibitor Studies

Cell Attachment, spreading, and invasion assays were performed in α 12- and QL α 12-MDCK cells (\pm dox) and \pm Src inhibitor (PP2 at 10 μ M) or the Rho kinase inhibitor (Y27632, 10 μ M) or phosphatase inhibitor (sodium orthovanadate at 100 μ M). The inhibitors were added immediately after the cells were detached and kept in the suspension of detached cells for 30 min before replating and analysis in the different assays. Attachment, spreading, and invasion were performed as described above images for figures assembled in Adobe Photoshop and Illustrator (Adobe Systems, San Jose, CA) as described.

Stable Knockdown of α 12 in MDCK Cells

α 12-specific siRNAs (forward: 5'-GATCCCCGGCATTGTGGAACATGACTCAAGAGATGCATGTTCCACAATGCCCTTTTGGAAA-3'; reverse: 5'-AGCTTTTCCAAAAAGGGCATTGTGGAACATGACTCTCTTGAAGTCA-TGTTCCACAATGCCCGGG-3') were cloned in to pSUPER vector using BglII and HindIII sites and standard techniques. A control pSUPER vector construct containing 64mer green fluorescent protein (GFP)-specific siRNA was used as negative control. In a ratio of 1:9, pSUPER vector (si α 12 or control) was cotransfected with blasticidin resistance plasmid using FuGENE 6 (Roche) according to the manufacturer's instructions. After overnight incubation, selective medium containing 10 ng/ μ l blasticidin was added to the medium. Stable transfectants were selected from individual clones after 4 wks of selection in the presence of blasticidin. RNA isolation of sh α 12 or short hairpin (sh)GFP-silenced MDCK cells was obtained by TRIzol (Invitrogen). Total RNA was purified according to the manufacturer's protocol and quantified. Five micrograms of total RNA was reverse-transcribed using the Transcriptor Reverse Transcriptase Kit (Roche). Equal aliquots of cDNA were subsequently amplified for β -actin and α 12. The oligonucleotide primer sequences used for β -actin and α 12 were as follows: β -actin: sense, 5'-CGCTAGTTGTAGATAACGGCTC-3'; antisense, 5'-GCTTGCTGATCCACATCTGCTG-3'; and α 12: sense, 5'-GTTCTGTGCGATGCCCGAGACA-3'; antisense, 5'-TCACTGCAGCATGATGTCCTC-3'. After 30 cycles, the amplified fragments were resolved by electrophoresis on a 1% agarose gel and visualized by ethidium bromide staining using a Kodak DC290 zoom digital camera.

3D Tubulogenesis Assay

Tubulogenesis assays were performed according to the method of Pollack *et al.* (1998). Briefly, cells were grown to 60–80% confluence on 10-cm² dishes, trypsinized, and resuspended at a concentration of 4×10^4 cells/ml in collagen-I, 10 \times DMEM, and HEPES (at 8:1:1) on ice. The single-cell suspension was plated on to slide chambers for 30 min at 37°C and allowed to solidify. Two milliliters of 10% FBS in tissue culture media with or without HGF (20 ng/ml; Sigma) was then placed on top. The medium was replaced every 2 d, cultures were photographed at 7 d, and images were assembled in Adobe Photoshop and Illustrator (Adobe Systems). For experiments with α 12- and QL α 12-MDCK cells, parallel cultures were established \pm dox (40 ng/ml).

Staining of MDCK Cells Cultured in 3D Collagen Gels

3D cultures were prepared as described above and then washed three times with PBS. 3D cultures were treated with collagenase (type VII 7, 500 U) for 10 min at 37°C. Slides were washed three times with PBS and fixed with 4% PFA for 30 min (with gentle shaking). Slides were washed three times with PBS followed by blocking buffer (1.6 ml 45% gelatin from cold water fish skin, Sigma; 1.25 ml saponin, Calbiochem in 100 ml PBS) for 30 min at RT. Slides were then stained with rat mAb to E-cadherin (Abcam, Cambridge, MA) at 1:50 in PFS at 4°C overnight. Slides were washed three times with PBS and incubated with Alexa 488 goat anti-rat IgG 1:1000 in blocking buffer overnight. Images were obtained using a Nikon confocal microscope, and images were assembled using Adobe Photoshop and Illustrator.

Quantification and Statistics

Western blots were scanned using an Epson 1640 desktop scanner (Long Beach, CA), and band intensity quantified using NIH Image (Wayne Rasband) after subtracting background and determining linear range. Statistics were done in GraphPad Prism (San Diego, CA). Significance was determined by using *t* test.

RESULTS

α 12 Regulates MDCK Cell Interactions with Collagen-I through $\alpha 2\beta 1$ Integrin

MDCK cells with inducible (Tet-off) expression of α 12 or constitutively active α 12 (QL) have been previously characterized (Meyer *et al.*, 2002, 2003; Yanamadala *et al.*, 2007; Sabath *et al.*, 2008). Figure 1A shows the inducible α 12 expression at 48 h after removal of doxycycline ($-$ dox) in both α 12- and QL α 12-MDCK cells. During routine culturing, we noticed that QL α 12-MDCK cells in $-$ dox were less adherent to the plate. To determine if this depended on the substrate, we tested the interactions of control (Tet-off), wild-type α 12-MDCK, and QL α 12-MDCK cells \pm dox for interaction with various extracellular matrix components (Figure 1 and Supplemental Figure S1). BSA was used as a protein control for non-integrin-mediated interactions. Figure 1 shows attachment of Tet-off, α 12-, and QL α 12-MDCK cells \pm dox to collagen-I (Figure 1B), collagen-IV (Figure 1C), laminin-1 (Figure 1D), and fibronectin (Figure 1E). The attachment of MDCK cells to collagen-I was significantly reduced (58% of control) with α 12 expression ($-$ dox, Figure 1B) and with expression of activated α 12 (QL α 12, $-$ dox), attachment to collagen-I was further reduced (42% of control, Figure 1B). All of the MDCK cell lines interacted strongly with collagen-IV, but there was no demonstrable difference with α 12 or QL α 12 expression (Figure 1C). On laminin-1, each MDCK cell line was adherent but only with QL α 12 expression ($-$ dox) was there a significant loss of cell attachment (Figure 1D). In contrast, there was no specific binding of any of the MDCK cells \pm dox to fibronectin when compared with BSA (Figure 1E). Supplemental Figure S1 shows interactions of α 12-MDCK cells \pm dox with Matrigel (Supplemental Figure S1A) and laminin-5 (Supplemental Figure S1B), and vitronectin (Figure 1C). Matrigel is composed predominantly of laminin-1, and the interaction of α 12-MDCK cells on Matrigel was similar to what we observed with laminin-1 (Figure 1D). The adherence to vitronectin was similar to BSA and was not affected by α 12 or QL α 12 expression ($-$ dox; Supplemental Figure S1C). However, on laminin-5 we observed significant binding that was inhibited with QL α 12 expression ($-$ dox) but not with expression of wild-type α 12 (Supplemental Figure S1B). The findings with laminin-1, laminin-5, and Matrigel suggest α 12 regulation of other integrins in epithelial cell attachment. Because collagen-I is ubiquitously expressed in all major organs and there was α 12-dependent binding to collagen-I but not to collagen-IV, we focused our subsequent studies on $\alpha 2\beta 1$ integrin and collagen-I.

To extend the observations made with the Tet-inducible MDCK cells, we repeated the analysis using LLC-PK₁ (porcine kidney epithelial) cells with stable expression of wild-type α 12, QL α 12, or vector control (kindly provided by Lakshman Gunaratnam (Brigham and Women's Hospital, Boston, MA, unpublished data). Supplemental Figure S1D shows that similar to the inducible MDCK cells, overexpression of wild-type α 12 or QL α 12 in LLC-PK₁ cells led to significant loss of attachment to collagen-I, and the effect was more pronounced in QL α 12-expressing cells. To estab-

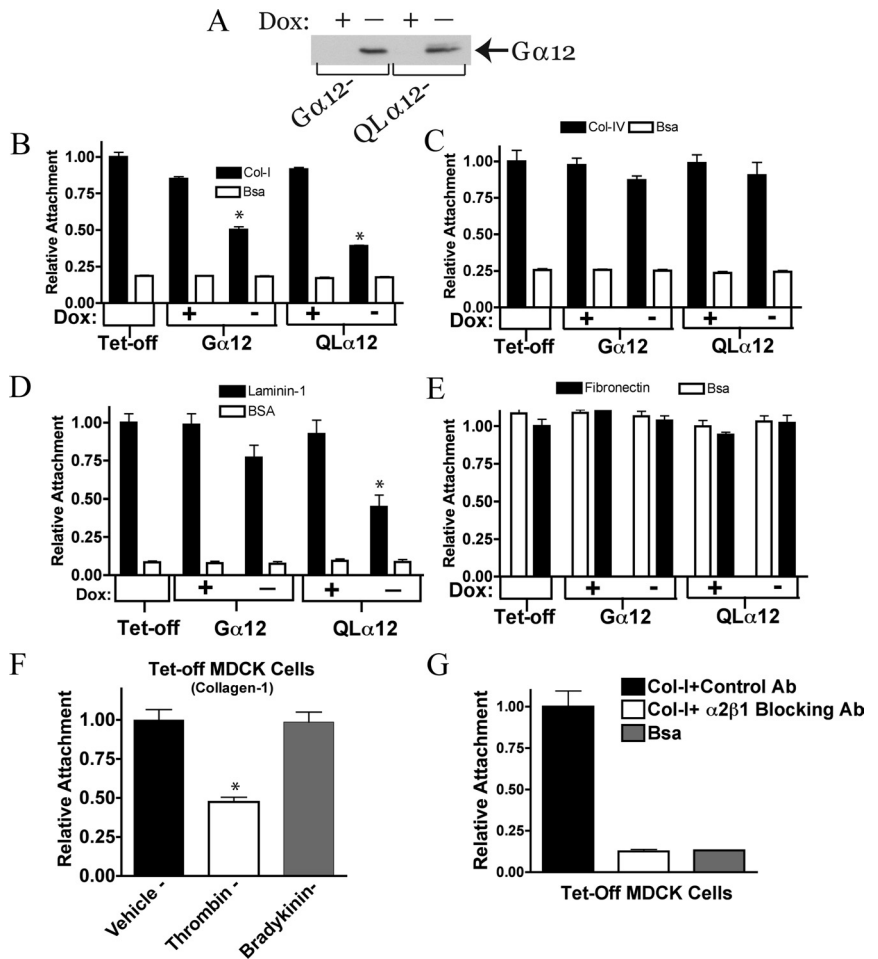


Figure 1. Attachment to collagen-I is inhibited with G α 12 activation. (A) Western blot showing inducible G α 12 and QL α 12 expression in \pm dox. G α 12- and QL α 12-MDCK cells were cultured \pm dox for 48 h before preparation of cell lysates and \sim 50 μ g total protein analyzed by SDS-PAGE and Western blot as described in *Materials and Methods*. Attachment to collagen-I (B), collagen-IV (C), laminin-1 (D), and fibronectin (E). Tet-off, G α 12-, and QL α 12-MDCK cells \pm dox were analyzed for attachment to various substrates as described in *Materials and Methods*. (F) Thrombin stimulates detachment in Tet-off MDCK cells. Identical numbers of Tet-off cells were stimulated with vehicle, thrombin (2 U/ml), or bradykinin (100 μ M) for 30 min after detachment and subsequent plating on collagen-I. Attachment was measured as described above. (G) MDCK cell attachment to collagen-I was completely inhibited by preincubation with α 2 β 1 integrin-blocking antibody (at 10 μ g/ml) and unaffected by a control antibody. Significance, * p < 0.05.

lish that MDCK cell attachment to collagen-I can be regulated by endogenous G α 12 signaling pathways, Tet-off cells were treated with vehicle, thrombin, or bradykinin for 30 min before the cell-attachment assay. Thrombin activates both G α 12 and G α 13, but bradykinin activates G α 13 (Riobo and Manning, 2005; Sabath *et al.*, 2008). Therefore, effects seen with thrombin, but not bradykinin, are consistent with activation of G α 12-signaling pathways. Figure 1F shows that bradykinin had no significant effect on cell attachment, but thrombin stimulation led to significant loss of attachment (\sim 50%). To confirm the requirement of α 2 β 1 integrin in mediating MDCK cell attachment to collagen-I, the cell attachment experiments were repeated in the presence and absence of an antibody that blocks α 2 β 1 integrin signaling (Wang and Frazier, 1998; Figure 1G). Absolute binding of MDCK cells to collagen-I in the presence of the control antibody was nearly identical to no added antibody conditions (not shown). However, cell attachment to collagen-I for Tet-off MDCK cells preincubated with α 2 β 1 integrin blocking antibody was completely inhibited and indistinguishable from BSA controls (Figure 1G). Control experiments assessing cell viability in the presence of each of these antibodies found there was no detectable cell death under these conditions (not shown). Similar results were seen with the G α 12- and QL α 12-MDCK cells in +dox (not shown). Taken together, these studies reveal G α 12-regulated MDCK cell interactions with collagen-I require α 2 β 1 integrin.

Activation of G α 12 in MDCK Cells Cultured on Collagen-I Leads to Loss of Lamellipodia and Focal Adhesions

To further characterize the effect of G α 12/ α 2 β 1 integrin signaling on MDCK cell phenotypes cultured on collagen-I, we compared MDCK cells with inducible expression of G α 12 and QL α 12 with Tet-off cells in cell spreading and migration assays. To examine cell spreading, cells were dissociated from a confluent monolayer and imaged 30 min after plating on to collagen-I. Figure 2A shows that control cells (Tet-off, G α 12 +dox, and QL α 12 +dox) develop cellular extensions and a flattened appearance within 30 min. However, in G α 12- or QL α 12-expressing cells ($-$ dox) there was little or no cytoplasmic extension, and only the nuclei were visible in most cells. To further examine focal adhesions under these conditions, we stained subconfluent MDCK cells for vinculin. Figure 2B shows that vinculin is present in numerous focal adhesion complexes in Tet-off, G α 12-, and QL α 12-MDCK cells in +dox. With wild-type G α 12 expression ($-$ dox; Figure 2B) vinculin staining was reduced but was still present in some areas (white arrow). With QL α 12 expression, the normal pattern of vinculin staining was significantly altered with nearly complete loss of staining (arrowheads). This finding suggests that QL α 12 activation of α 2 β 1 integrin on collagen-I leads to defects in focal adhesion and lamellipodia formation. However, G α 12 expression (wild type and QL in $-$ dox) still led to increased actin stress fiber formation as expected from activation of Rho pathways (Figure 2C and see Figure 6A).

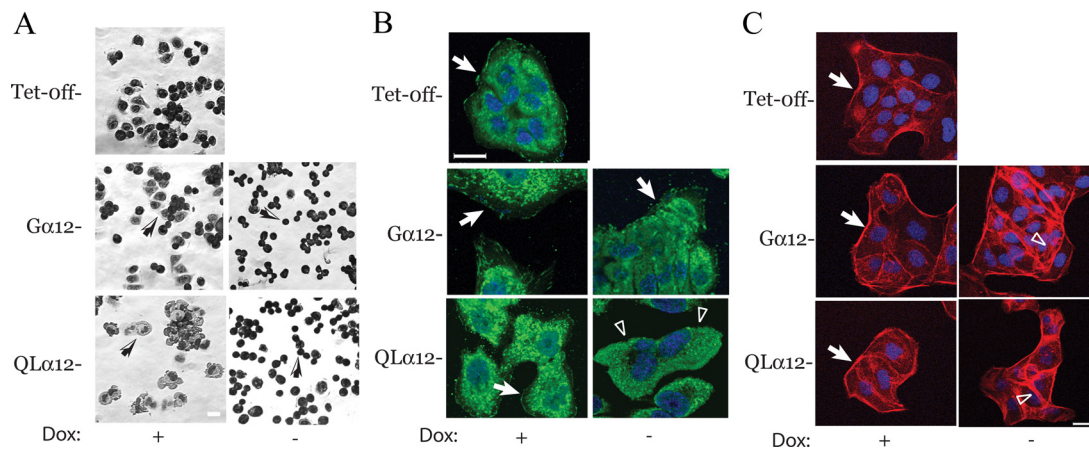


Figure 2. Cell spreading and focal adhesions are inhibited with $G\alpha 12$ activation. (A) Tet-off, $G\alpha 12$ -, and $QL\alpha 12$ -MDCK cells cultured \pm dox for 72 h were detached as described in the Materials and Methods plated on to collagen-I coated plastic at $T = 0$. Cells were fixed and stained with Giemsa at $T = 30$ min. Arrows denote stained cells in the various conditions and small rounded cells were seen with in $G\alpha 12$ - and $QL\alpha 12$ -MDCK cells in $-$ dox. (B) Vinculin staining of Tet-off and $G\alpha 12$ -, $QL\alpha 12$ -MDCK cells \pm dox. Arrows denote punctate focal adhesion staining in the controls (Tet-off and $+dox$). Arrowheads in $QL\alpha 12$ -dox shows lack of focal adhesions. (C) Phalloidin staining of Tet-off and $G\alpha 12$ -, $QL\alpha 12$ -MDCK cells in \pm dox. Arrows show actin at leading edge of lamellipodia in Tet-off and $G\alpha 12$ - and $QL\alpha 12$ -MDCK cells in $+dox$. Open arrow heads indicate increased stress fibers in $G\alpha 12$ - and $QL\alpha 12$ -MDCK in $-dox$.

Activating $G\alpha 12$ Impairs Cell Migration

Epithelial cell migration is necessary for renal tubule development, and recent studies showed defective directed cell migration in $G\alpha 12/13$ knockout fibroblasts (Goulimari *et al.*, 2005). To determine if the impairment in cell spreading and focal adhesion formation affected cell migration, we examined two different contexts of migration: invasion assays, which are subconfluent cells migrating through a porous filter (8 μm ; see arrows in Figure 3A) and scratch wound assays (Figure 3, B–E). In the invasion assay, MDCK cells were cultured on the apical surface of the filter with HGF in the media. Cells that traverse the filter were visualized on the opposite surface of the filter after 18 h. An identical number of cells were plated in each condition. As shown in Figure 3A, left, Tet-off cells, $G\alpha 12$ -, and $QL\alpha 12$ -MDCK cells in $+dox$ readily migrated across the filter to the opposite side. With $G\alpha 12$ or $QL\alpha 12$ expression ($-dox$), $<5\%$ of cells migrated through to the opposite surface and the comparative results for each of these conditions are summarized in the bar graph (Figure 3a, right).

To examine cell migration in the context of a confluent monolayer, MDCK cells were analyzed on collagen-I in scratch-wound assays. $G\alpha 12$ - and $QL\alpha 12$ -MDCK cells \pm dox were analyzed by videomicroscopy after wounding at time = 0. Figure 3, B and C, shows representative images at 4, 12, 16, and 24 h after wounding for each condition, and the movies are provided as Supplemental Files (Supplemental Figure S3 and Movies 1–6). The relative closure rates were calculated by measuring the area of the gap at multiple time points. The areas were plotted versus time to calculate the slope (the rate of closure for each condition expressed as a percentage of the wound area) and then normalized to the $+dox$ control (black bars in Figure 3E). For all conditions, there was excellent fit for a linear relationship with $R^2 > 0.8$. Expressing wild-type $G\alpha 12$ or $QL\alpha 12$ led to closure rates about fourfold slower than the controls. The actual rates of closure are shown in Supplemental Table S1. To confirm that activation of endogenous $G\alpha 12$ -coupled pathways also resulted in delayed scratch-wound closure, the analysis was repeated utilizing Tet-off MDCK cells \pm thrombin. Similar to $G\alpha 12$ -MDCK cells \pm dox, Tet-off cells \pm thrombin also

closed the gap significantly more slowly with thrombin treatment (Figure 3, D and E). Although the absolute rates of closure were similar for the $G\alpha 12$ - and $QL\alpha 12$ -MDCK cells in $+dox$, they closed the gap more slowly than in Tet-off cells (Supplemental Table S1), possibly representing some leaky $G\alpha 12$ expression. Analysis of the movies suggests that the cells at the leading edge of the wound in the $G\alpha 12$ -expressing or thrombin-treated cells were impaired in their ability to extend lamellipodia and is consistent with the phenotypes described above. To exclude the possibility that there were changes in cell proliferation or apoptosis rates in cells lining the edge of the wound, TUNEL and bromodeoxyuridine incorporation were performed at 12–24 h after wound healing. No significant differences in proliferation or apoptosis were observed (results not shown).

Knockdown of $G\alpha 12$ in MDCK Cells Leads to Increased Attachment and Accelerated Spreading on Collagen-I

$QL\alpha 12$ expression in MDCK cells or thrombin stimulation of endogenous $G\alpha 12$ inhibited $\alpha 2\beta 1$ integrin function and cell attachment to collagen-I. To confirm the essential role for $G\alpha 12$ on this phenotype, we established MDCK cells with stable knockdown of endogenous $G\alpha 12$ (Figure 4). Canine $G\alpha 12$ was stably knocked down in MDCK cells using short hairpin RNA (shRNA) and compared it with a control cell line transfected with shRNA for GFP selected under identical conditions. Because endogenous $G\alpha 12$ is not detectable in MDCK cell lysates by Western analysis, we utilized RT-PCR to assess the knockdown efficiency. Figure 4A shows the results of RT-PCR for $G\alpha 12$ and actin in $G\alpha 12$ knockdown (sh $G\alpha 12$ -MDCK) and control cell lines (shRNA for GFP). $G\alpha 12$ mRNA levels were $\sim 16 \pm 8\%$ of the GFP control when normalized to the simultaneous β -actin control. Comparison of the sh $G\alpha 12$ -MDCK cells with shGFP and Tet-off controls revealed significantly increased attachment to collagen-I in the sh $G\alpha 12$ -MDCK cells (Figure 4B). In addition, when the cell lines were analyzed for cell spreading after plating on to collagen-I, the control cells were still quite rounded and revealed few cellular extensions when compared with the sh $G\alpha 12$ -MDCK cells imaged at the same time (Figure 4C).

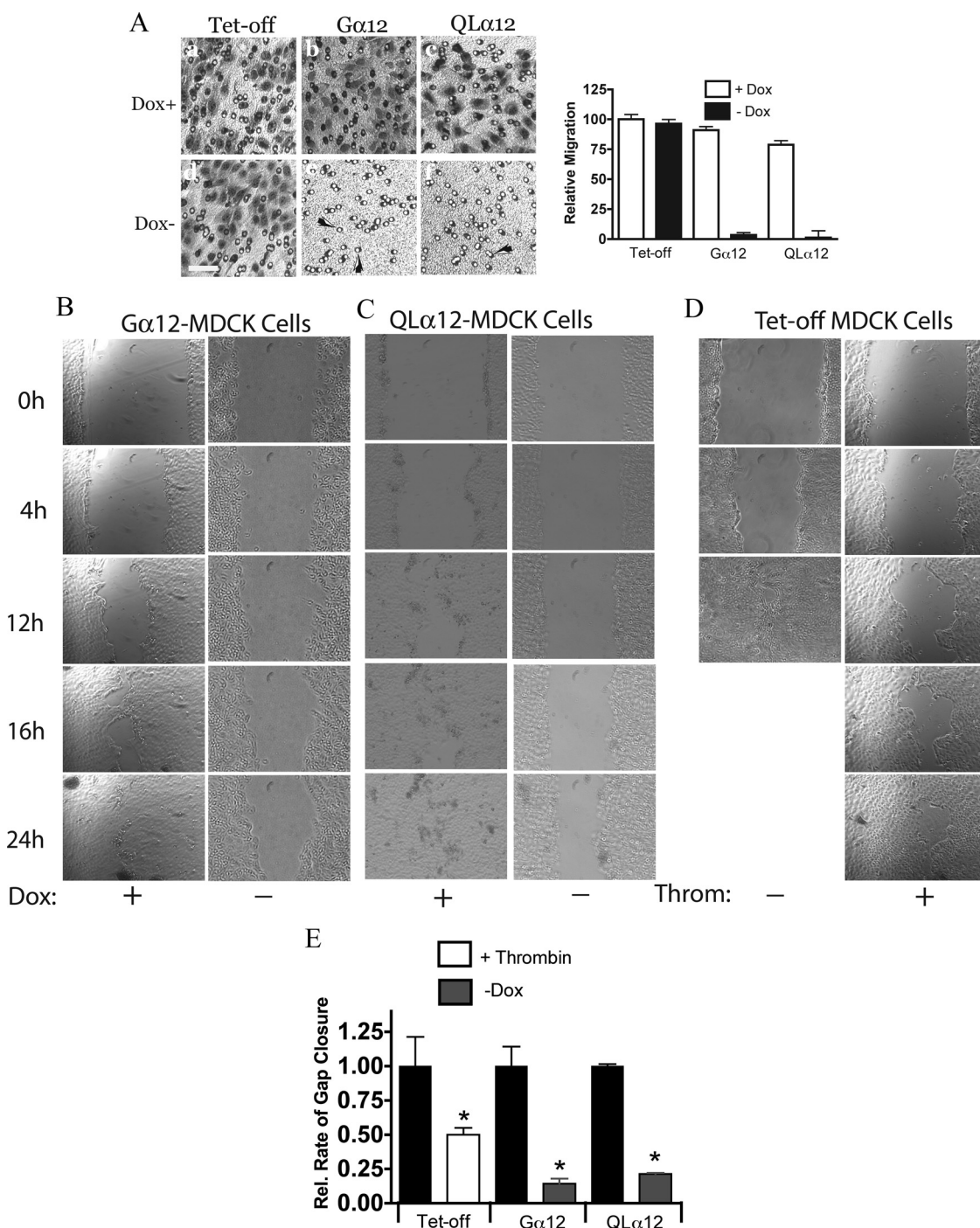


Figure 3. MDCK cell migration through a permeable membrane and in wound assays is inhibited with Gα12 activation. (A) Left (a–f), migration through Transwell filters. Equivalent numbers Tet-off, Gα12-, and QLα12-MDCK cells in ± dox were plated into the apical chamber of collagen-I-coated Transwell filters (8 μm) as described in *Materials and Methods*. Cultures were incubated at 37°C overnight, and the basal surface of the filter fixed and stained for migrating cells. Arrows mark pores within the surface of the filter. There were virtually no cells visualized in the Gα12 and QLα12 –dox conditions in comparison to the controls (e, f). Right, to quantify the relative migration, the number of cells visualized on the basal surface in 10 separate fields were counted and divided by the starting number of cells. Tet-off in +dox was used for the reference and set at 100. (B–D) Wound assays were performed as described in *Materials and Methods* for Gα12-MDCK ± dox (B) and QLα12-MDCK cells ± dox (C), and Tet-off cells ± 2 U/ml thrombin (D) were added at time = 0. Images from specific times for each cell line are shown and the average open area calculated using Image J at each time point. For Tet-off cells without thrombin, the gap was closed by approximately 12 h. (E) The relative rates of closure for each condition. For Tet-off: ■, –thrombin; □, + thrombin, which were set to 100%. The effect of thrombin (□) and Gα12 or QLα12 expression (–dox, ▨) is shown relative to the control (+dox, ■). Error bars are 95% confidence intervals for n = 2–3 experiments for each condition.

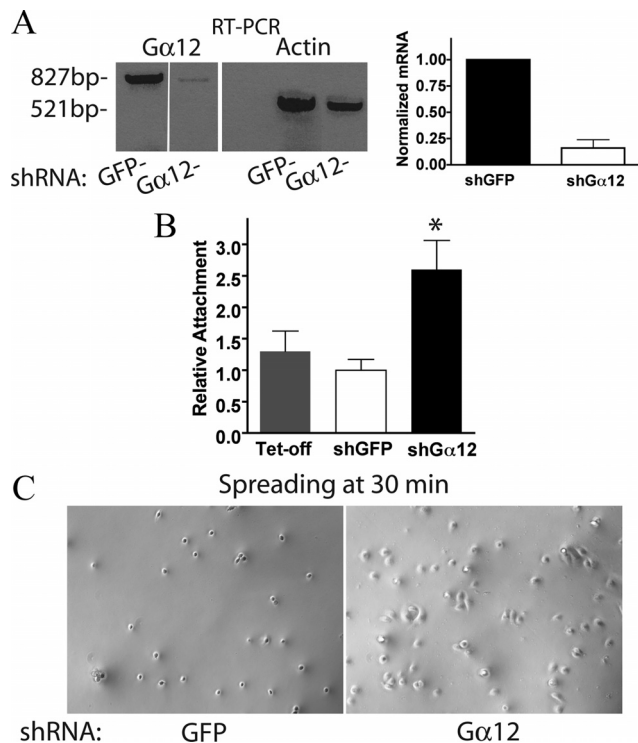


Figure 4. Silencing $G\alpha 12$ in MDCK cells increases attachment to collagen-I. (A) RT-PCR results of knockdown of $G\alpha 12$ in stable cell line transfected with shRNA for $G\alpha 12$ or control GFP shRNA as described in *Materials and Methods*. The $G\alpha 12$ transcript was normalized to β -actin for each condition and reveals $16 \pm 8\%$ of the control $G\alpha 12$ mRNA levels. (B) Attachment to collagen-I was compared for Tet-off, sh $G\alpha 12$ -, and shGFP-MDCK cells as described above. Results were normalized to Tet-off condition. $n = 3$ and significance at $*p < 0.02$. (C) Photomicrographs of phase-contrast images from GFP control and silenced $G\alpha 12$ -MDCK cells taken 30 min after plating on collagen-I.

Gα12 Activation Disrupts α2β1 Integrin Localization without Affecting Protein Levels

We next performed a series of experiments to define the effects of $G\alpha 12$ activation on $\alpha 2\beta 1$ properties. To determine if $G\alpha 12$ is a component of the integrin protein complex, we attempted double staining of $G\alpha 12$ -MDCK cells \pm dox with $G\alpha 12$ and $\alpha 2$ or $\beta 1$ integrin antibodies and imaging by confocal microscopy. The $G\alpha 12$ antibody does not work well in immunofluorescence microscopy, and in numerous double-staining experiments we were unable to identify conditions that revealed any significant colocalization of $G\alpha 12$ with the integrins (not shown). Likewise, immunoprecipitation of $\alpha 2$ integrin coprecipitates some detectable $G\alpha 12$, but we were not successful with the reverse immunoprecipitations (results not shown). Therefore, we are unable to definitively determine whether $G\alpha 12$ is part of the integrin protein complex. However, subsequent experiments clearly identify $G\alpha 12$ regulation of the focal adhesion complex (see Figures 6 and 7). We next quantified cell surface expression of $\alpha 2$ and $\beta 1$ integrins with $G\alpha 12$ expression (Figure 5A). Tet-off, $G\alpha 12$ -, and $QL\alpha 12$ -MDCK cell lines (\pm dox) were analyzed by FACS using specific antibodies to the extracellular domain for $\alpha 2$ and $\beta 1$ integrins. As shown in Figure 5A, the amount of integrin membrane expression (as determined by the position of the peak along the x -axis) was not significantly different in any of the tested cell lines under control conditions (Tet-off, $G\alpha 12$, and $QL\alpha 12$ +dox). Induc-

ing expression of $G\alpha 12$ or $QL\alpha 12$ for 48 h also had no effect on integrin membrane expression ($G\alpha 12$ - and $QL\alpha 12$ -MDCK cells -dox), indicating that changes in integrin expression were unlikely to account for the effects of $G\alpha 12$ activation. We next examined the localization of $\alpha 2$ and $\beta 1$ integrins with $G\alpha 12$ expression. $G\alpha 12$ - and $QL\alpha 12$ -MDCK cells (\pm dox) were stained for $\alpha 2$ or $\beta 1$ integrin and analyzed by immunofluorescent microscopy (Figure 5B). Most $\alpha 2$ and $\beta 1$ integrins were found in the plasma membrane of MDCK cells in the control conditions (+dox). With expression of $G\alpha 12$, $\alpha 2$ and $\beta 1$ integrins appeared slightly more diffuse along the cell membrane in -dox when compared with the control (+dox; Figure 5B). In $QL\alpha 12$ (-dox), $\alpha 2$ and $\beta 1$ integrins appeared more diffusely localized along the membrane, suggesting that the integrin localization in the plasma membrane had been altered with $G\alpha 12$ expression. To determine whether the altered staining pattern reflected changes to integrin interactions with the actin cytoskeleton, we performed Triton X-100 extractions of the monolayers. We did not detect any significant differences in solubility of $\alpha 2$ and $\beta 1$ integrins (not shown), and this suggests that $G\alpha 12$ activation did not significantly affect integrin-cytoskeletal interactions. However, $G\alpha 12$ activation did result in disruption of $\alpha 2$ integrin/FAK interactions (see Figure 6).

Gα12 Regulates Cell Attachment and α2/FAK Interactions through Rho and Src Pathways

$G\alpha 12$ and integrin signaling both utilize Rho and Src tyrosine kinase pathways. To determine whether these pathways were important in $G\alpha 12/\alpha 2\beta 1$ integrin signaling, we examined these downstream molecules in this model. Using $G\alpha 12$ - and $QL\alpha 12$ -MDCK cells \pm dox on collagen-I, Rho activity was determined by glutathione S-transferase (GST)-Rhotekin pulldowns and Src activity assessed by Western analysis to phospho-tyrosine 418 (Figure 6, A and B). Rho activity was increased with $G\alpha 12$ or $QL\alpha 12$ expression, and activation was greater in $QL\alpha 12$ -MDCK cells. This finding was in contrast to our previous studies on Rho activity in these cells (Meyer *et al.*, 2003) and may reflect the requirement for collagen-I in the extracellular matrix. There was some endogenous Rho activation in $QL\alpha 12$ -MDCK cells in +dox, possibly indicating some leaky $QL\alpha 12$ expression. As we previously reported, Src activity (as determined by pTyr-418 Western blot intensity) was increased $\sim 40\%$ in $QL\alpha 12$ -MDCK cells (Figure 6B), with only subtle changes in $G\alpha 12$ -MDCK cells \pm dox. This degree of stimulation by $QL\alpha 12$ is similar to what was previously observed (Meyer *et al.*, 2003; Sabath *et al.*, 2008). To establish that Rho and Src signaling were important to $G\alpha 12$ -stimulated loss of attachment to collagen-I, the cell attachment and spreading experiments were repeated in the presence and absence of the Rho kinase (ROCK) inhibitor Y27632 and the Src inhibitor PP2. Figure 6C shows that inhibiting ROCK with Y27632 completely prevented the $QL\alpha 12$ -stimulated loss of attachment to collagen-I, and PP2 had a partial effect. Likewise, with $QL\alpha 12$ expression in the presence of Y27632, the cell spreading appearance was similar to the control (+dox, no inhibitors, Figure 6D). Similar to the attachment assay, there appeared to be a partial normalization of the spreading phenotype with PP2. In LLC-PK₁ cells expressing $G\alpha 12$ and $QL\alpha 12$, inhibiting Rho reversed the loss of attachment and Src inhibitors had a partial effect (Supplemental Figure S2A). Supplemental Figure S2B shows that cell spreading was also affected in $G\alpha 12$ - and $QL\alpha 12$ -transfected cells, and the findings were similar to the MDCK cell model. Next, we examined the $\alpha 2$ integrin/FAK protein complex in these cells by immunoprecipitating $\alpha 2$ integrin and looking for coprecipi-

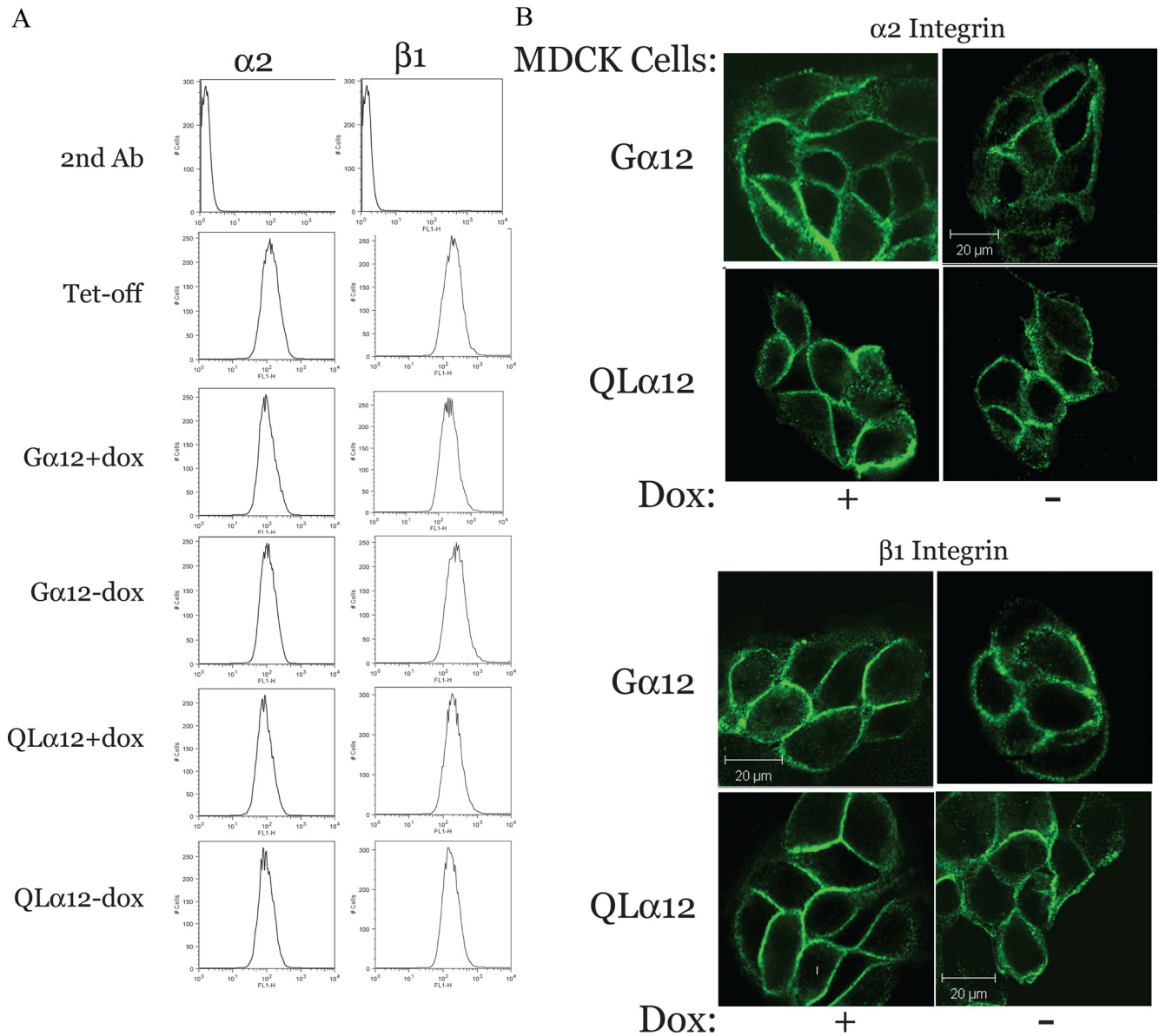


Figure 5. $\alpha 2$ and $\beta 1$ integrin membrane localization is altered with QL $\alpha 12$ expression without affecting membrane expression. (A) Membrane expression of integrins. Tet-off, G $\alpha 12$ -, and QL $\alpha 12$ -MDCK cells were cultured \pm dox for 72 h and then surface-labeled with antibodies to $\alpha 2$ and $\beta 1$ integrins as described in *Materials and Methods*. Cells were then analyzed by FACS and sorted by intensity for specific integrin staining. The position along the X-axis reflects the amount of surface labeling and was not significantly different in any of the conditions. (B) Immunofluorescence microscopy of $\alpha 2$ and $\beta 1$ integrins. G $\alpha 12$ - and QL $\alpha 12$ -MDCK cells (\pm dox) were stained with specific antibodies and imaged as described in *Materials and Methods*. Bar, 20 μ m.

tated FAK. Figure 6E shows that FAK is precipitated with $\alpha 2$ integrin in each condition except for QL $\alpha 12$ -dox. This is consistent with loss of the $\alpha 2$ integrin-FAK interaction with QL $\alpha 12$ expression and would account for the loss of attachment and spreading with G $\alpha 12$ activation. Controls with a nonspecific antibody (4F2) did not precipitate FAK. To determine whether the disruption of the $\alpha 2$ integrin-FAK complex was mediated by Rho and/or Src pathways, we repeated the experiment in the presence and absence of the Rho kinase inhibitor, Y27632, or the Src family kinase inhibitor, PP2, for each cell line. Pretreatment of the cells with either inhibitor prevented G $\alpha 12$ -stimulated loss of the complex (Figure 6E). In addition, it appeared that inhibiting Rho kinase led to stabilization of the $\alpha 2$ integrin-FAK complex

compared with untreated (left panel) or PP2 treated for each cell line except QL $\alpha 12$ in +dox.

G $\alpha 12$ Regulates FAK and Paxillin Phosphorylation: Evidence for Activation of a Tyrosine Phosphatase

To gain insights into the mechanisms of G $\alpha 12$ regulation of MDCK cell migration, a phosphoprotein screen (Kinexus, Vancouver, BC, Canada) was performed on QL $\alpha 12$ -MDCK cells in \pm dox and was previously described (Yanamadala *et al.*, 2007). This screen revealed decreased tyrosine phosphorylation of paxillin (pTyr118) and FAK (pTyr397) in QL $\alpha 12$ -expressing MDCK cells (-dox, Figure 7A). To confirm and extend these results, we carefully examined FAK and paxillin tyrosine phosphorylation in Tet-off, G $\alpha 12$ -, and QL $\alpha 12$ -

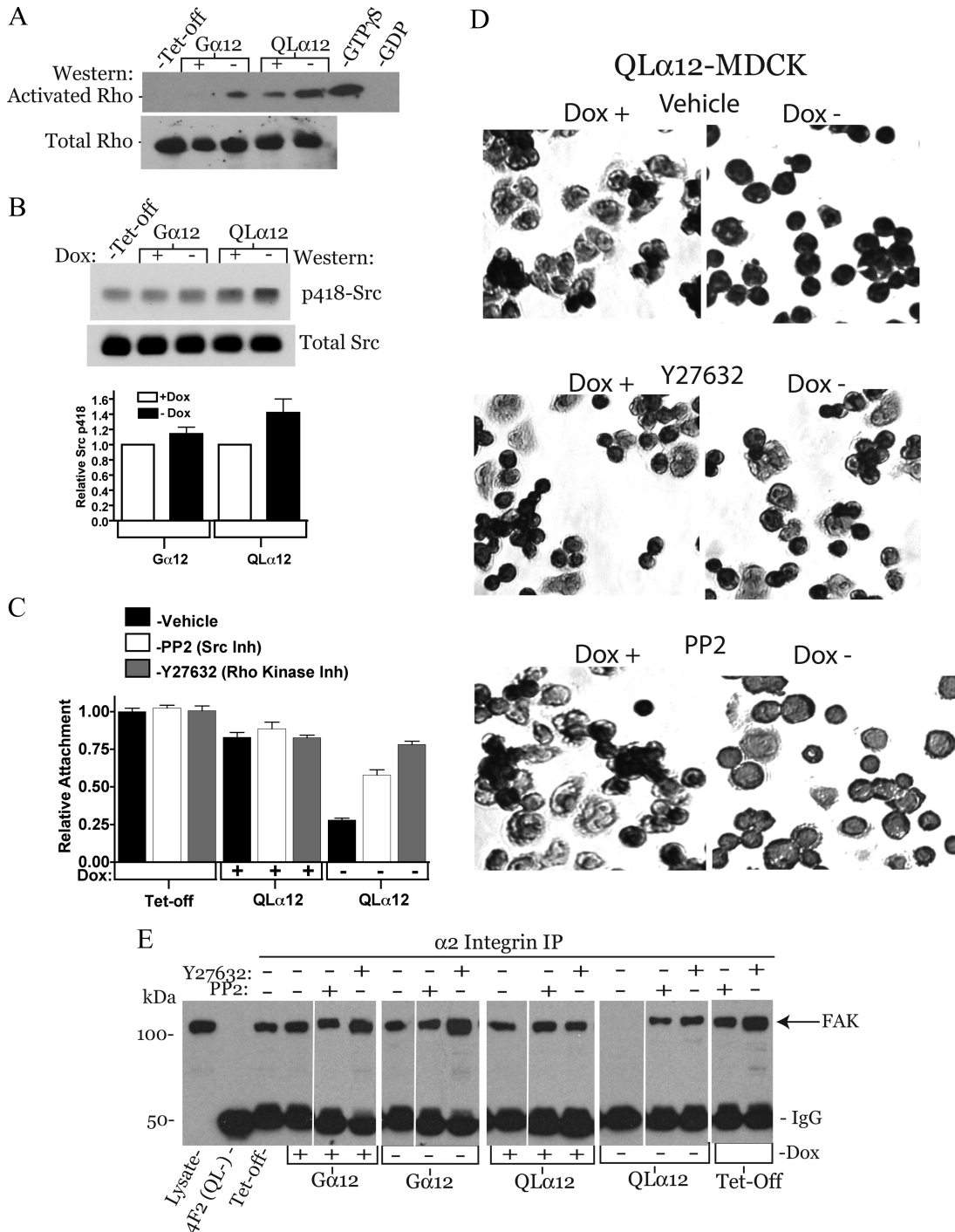


Figure 6. Rho and Src mediate Gα12-stimulated decreased attachment and disruption of the α2 integrin/FAK complex. (A) Rho activation in Tet-off, Gα12-, and QLα12-MDCK cells ± dox. Rho activity was determined using Rhotekin GST pulldowns as described in *Materials and Methods*. Cell lysates from control cells were incubated with GDP (1 mM, negative control) or GTPγS (200 μM, positive control). Pulldowns were analyzed for Rho by Western blot and lysates (~50 μg) analyzed for total Rho. (B) Src tyrosine kinase activity in Tet-off, Gα12-, and QLα12-MDCK cells ± dox. Approximately 50 μg of cell lysate was analyzed by Western blot for p-Tyr-418 and total Src. The results of two independent experiments are summarized in the bar graph; error bars, range. (C) Cell attachment to collagen-I for QLα12-MDCK cells ± dox treated with the Rho kinase inhibitor (Y27632) or the Src inhibitor (PP2). (D) Cell spreading of QLα12-MDCK cells ± dox cultured on collagen-I in the presence and absence of vehicle, Y27632, and PP2. Cells were detached, inhibitors were added, and cells were plated on collagen-I for 30 min, followed by fixation and nuclear staining with Giemsa. The loss of cellular extensions seen in -dox was inhibited with Rho kinase inhibition and partially with Src inhibition. (E) Activating Gα12 leads to disruption of α2 integrin and FAK complex in a Rho and Src-dependent manner. Tet-off, Gα12-, and QLα12-MDCK cells ± dox were immunoprecipitated with 5E8 antibody to α2 integrin and then analyzed by Western blot for coprecipitating FAK (arrow). All of the lanes are assembled from the same gel and exposure. White lines indicate where conditions were regrouped. There is no detectable FAK in the α2 integrin immunoprecipitation from QLα12-MDCK cells in -dox, and there was no detectable FAK precipitating with a nonspecific antibody (4F2). When the cells were preincubated with the Rho kinase inhibitor (Y27632) or the Src inhibitor (PP2), the interaction of α2 integrin and FAK was preserved.

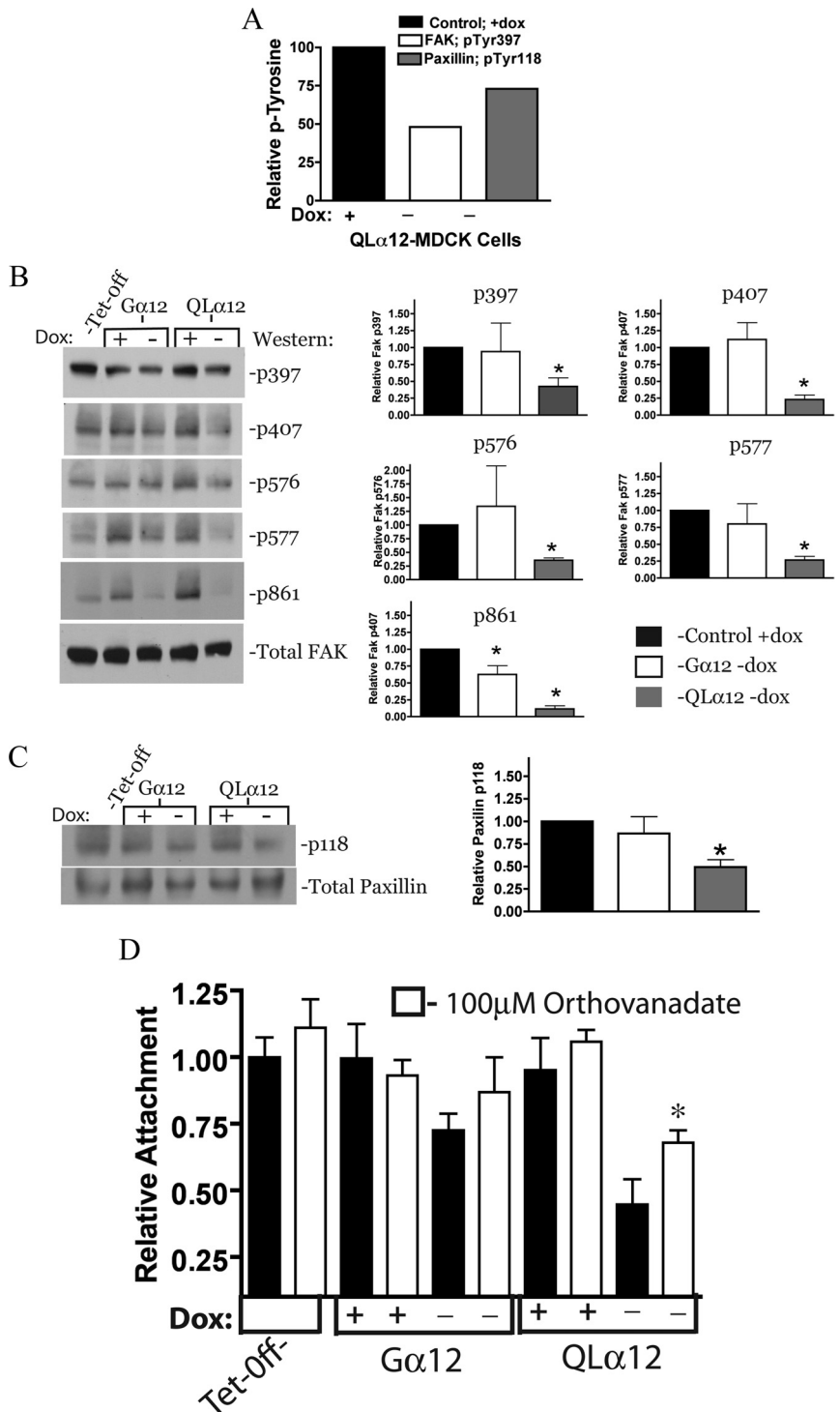


Figure 7. α 12 stimulates loss of FAK and paxillin phosphorylation and attachment is partially restored with protein phosphatase inhibition. (A) Results of the phosphoprotein screen (Kinexus) for QL α 12-MDCK cells \pm dox. Relative to +dox, in QL α 12-expressing MDCK cells (-dox), there was a 52% reduction in pTyr-397 FAK phosphorylation and a 27% reduction in pTyr 118 of paxillin. (B) Left, FAK is dephosphorylated with α 12 activation. Tet-off, α 12-, and QL α 12-MDCK cells \pm dox were analyzed in triplicate, and representative Western blots for each FAK phosphorylation are shown. Right, bar graphs summarize three independent experiments (mean \pm SEM) for each phosphorylation site and are normalized to the +dox condition. (C) Left, paxillin p118 phosphorylation is reduced with QL α 12 expression and a representative Western is shown; right, the bar graph shows the mean \pm SEM for three independent experiments. (D) QL α 12-stimulated loss of cell attachment to collagen-I is partially reversed with sodium orthovanadate. Tet-off, α 12-, and QL α 12-MDCK cells \pm dox were pretreated with sodium orthovanadate (100 μ M) for 30 min after detachment and before measuring cell attachment on collagen-I.

MDCK cells \pm dox and then determined relative levels of pTyr at each site by Western blot with phospho-specific antibodies. Figure 7B shows that in QL α 12 -dox MDCK cells there was significant inhibition of FAK phosphorylation on all tested phosphorylation sites (pTyr397, pTyr407, pTyr576-577, and pTyr861). In MDCK cells expressing wild-type α 12, the effects were subtle, with only decreased phosphorylation on pTyr861 being significant. These findings are consistent with the partial phenotype seen in α 12-MDCK cells. For paxillin phosphorylation, there was a sig-

nificant decrease in pTyr118 in QL α 12-MDCK-expressing cells with no significant change in the α 12-MDCK cells (Figure 7C). The loss of important tyrosine phosphorylation on key residues of FAK and paxillin suggests that α 12-activated pathways include activation of a protein tyrosine phosphatase. To test for the potential role of a tyrosine phosphatase in α 12-stimulated MDCK cells grown on collagen-I, we examined MDCK cell adhesion to collagen-I in the presence and absence of sodium orthovanadate, a non-specific inhibitor of protein tyrosine phosphatases. Figure

7D shows that the inhibitor had minor effects on Tet-off, $G\alpha 12$ -, or $QL\alpha 12$ -MDCK cells in +dox. In -dox, the expected loss of attachment was seen in $G\alpha 12$ - and $QL\alpha 12$ -MDCK cells (similar to Figures 1 and 6). Pretreatment of $QL\alpha 12$ -MDCK in -dox with 100 μ M sodium orthovanadate partially (but significantly) rescued the attachment phenotype, and a smaller effect was seen in the $G\alpha 12$ -MDCK cells. Taken together, these findings are consistent with $G\alpha 12$ activation of Rho and Src signaling pathways that lead to activation of a protein tyrosine phosphatase(s), loss of tyrosine phosphorylation on FAK and paxillin, resulting in altered $\alpha 2\beta 1$ function and decreased attachment to collagen-I (see also Figure 9).

Stimulating $G\alpha 12$ Inhibits Tubulogenesis in 3D Culture and Leads to Formation of Cystic Structures

To test whether these mechanisms were important in a model of epithelial morphogenesis, we characterized the effects of $G\alpha 12$ activation on tubulogenesis using the MDCK cell 3D tubulogenesis assay. This model of tubule development utilizes collagen-I in the matrix and HGF stimulation and depends on several integrin families including $\alpha 2\beta 1$ integrin. $G\alpha 12$ - and $QL\alpha 12$ -MDCK cells \pm dox were cultured in 3D collagen-I with HGF for 7 d. Figure 8A shows that $G\alpha 12$ -MDCK cells formed branching tubules, and there were no significant differences in \pm dox (Figure 8A). In $QL\alpha 12$ -MDCK cells, tubulogenesis was similar to the $G\alpha 12$ control cells in +dox (Figure 8Ac), but with induction of $QL\alpha 12$ (-dox), very few tubular structures were identified, and nearly all structures appeared as large multicellular structures consistent with cysts (Figure 8Ad). To further define the cyst-like structures seen with $QL\alpha 12$ expression, confocal microscopy of E-cadherin stained 3D collagen-I gels was performed after 7 d in \pm dox. Figure 8B shows a branching structure in $QL\alpha 12$ +dox with E-cadherin staining outlining the tubule surface. With $QL\alpha 12$ expression (-dox), a circumferential ring of E-cadherin-positive cells lined the cyst with no detectable intracystic staining, consistent with a cell-free lumen surrounded by epithelial cells. To determine whether activation of endogenous $G\alpha 12$ regulates tubulogenesis, we utilized thrombin and bradykinin as described for Figure 1. Figure 8C shows that thrombin but not bradykinin significantly reduced the number of tubular structures and increased the number of cysts. However, the morphology of thrombin-stimulated cystic structures was subtly different from the $G\alpha 12$ -stimulated cysts (Figure 8Cb); they were slightly smaller and contained short linear extensions from the central body. To confirm that $G\alpha 12$ activation leads to impaired tubulogenesis and the formation of cystic structures, the 3D tubulogenesis assay was repeated using the sh $G\alpha 12$ -MDCK cells shown in Figure 8D. Control and $G\alpha 12$ -silenced MDCK cells were cultured \pm thrombin as described above. After 7 d, tubulogenesis was well developed in both the control cells and in $G\alpha 12$ -silenced MDCK cells in the absence of thrombin. With thrombin stimulation, the control cells formed cystic structures similar to those seen in Figure 8, A and C, but thrombin stimulated loss of tubulogenesis, and the formation of cystic structures was significantly reduced in the $G\alpha 12$ -silenced cells (Figure 8Dd). Taken together, these findings are consistent with those showing that activated $G\alpha 12$ inhibits tubulogenesis and promotes the formation of cystic structures.

DISCUSSION

Epithelial cell attachment and migration are required for numerous biological processes including organogenesis and

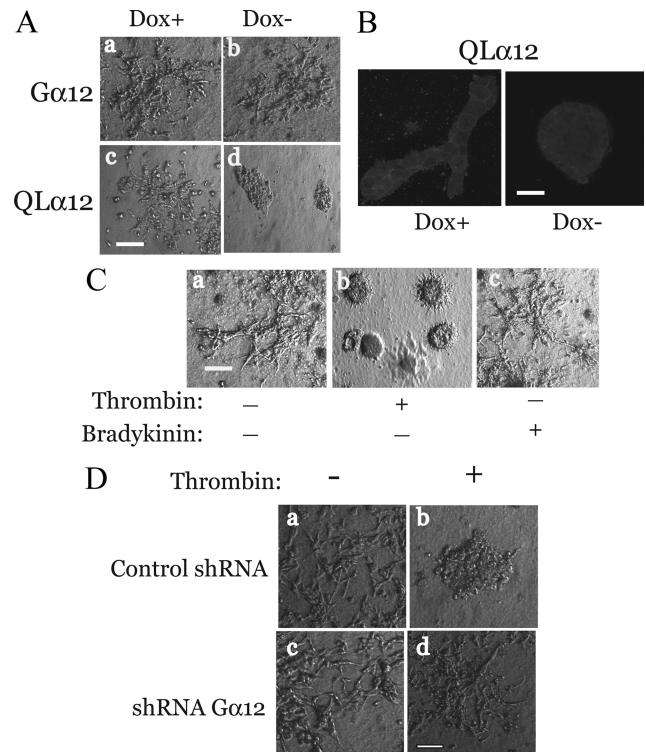


Figure 8. $G\alpha 12$ regulates tubulogenesis. (A) Tubulogenesis assay with $G\alpha 12$ - and $QL\alpha 12$ -MDCK cells \pm dox. $G\alpha 12$ - and $QL\alpha 12$ -MDCK cells \pm dox (4×10^4 cells) were trypsinized, washed, and mixed with 3D gel (3.5 mg/ml collagen-I, 20 ng/ml HGF with HEPES buffer in DMEM, and \pm dox) as described in *Materials and Methods*. Phase-contrast microscopy after 7 d in culture; (a) $G\alpha 12$ +dox; (b) $G\alpha 12$ -dox; (c) $QL\alpha 12$ +dox; and (d) $QL\alpha 12$ -dox. Representative images are shown. Bar, 100 μ m. (B) 3D cultures were stained with E-cadherin and imaged by confocal microscopy as described in *Materials and Methods*. Bar, 15 μ m. (C) Thrombin inhibits tubulogenesis assay in control MDCK cells (Tet-off). Tubulogenesis assay with Tet-off MDCK cells stimulated with (a) vehicle, (b) thrombin (2 U/ml), or (c) bradykinin (100 μ M) for 7 d. Bar, 100 μ m. (D) $G\alpha 12$ -silenced MDCK cells are resistant to cyst development. sh $G\alpha 12$ - and shGFP-MDCK cells (Control shRNA) were cultured \pm thrombin for 7 d in 3D tubulogenesis assay (a–d). Bar, 25 μ m.

recovery from acute injury. Furthermore, diseases that affect the signaling pathways utilized for attachment and migration contribute to metastatic potential in several epithelial cell cancers. The findings reported here reveal novel insights in to G protein regulation of integrins and have implications for understanding the development and maintenance of normal epithelial tissues. Expressing $G\alpha 12$ in MDCK cells mimics two epithelial cell cancers (prostate and breast) where $G\alpha 12$ expression was increased and correlated with metastatic potential (Kelly *et al.*, 2006a,b). Our finding of decreased cell attachment with overexpressing $G\alpha 12$, or activated $G\alpha 12$ (by QL mutation or through a G protein-coupled receptor) is likely to be an important mechanism contributing to the metastatic potential of these malignancies. Furthermore, the finding that $G\alpha 12$ activation inhibits tubulogenesis and leads to the development of cystic structures highlights the importance for $G\alpha 12$ /integrin signaling in epithelial development and suggests a potential role in the pathogenesis of cystic kidney diseases. Finally, these studies reveal a mechanism for $G\alpha 12$ /integrin-regulated interactions with the extracellular matrix. As summarized in Figure 9, an inside out signaling model is suggested, where

G α 12 regulates Rho and Src, resulting in decreased FAK phosphorylation and disruption of the α 2 integrin-FAK protein complex. This signaling mechanism is likely to account for the loss of cell attachment, decreased lamellipodia, impaired migration, and defective tubulogenesis seen with G α 12 activation.

Because G α 12 is difficult to detect in most cells, the use of the inducible MDCK cell model system has proven to be very useful for unraveling novel functions of G α 12 in epithelia. In these studies, we found that some phenotypes were indistinguishable between the overexpressing wild-type G α 12- and the QL α 12-expressing MDCK cells. For example, there were no detectable differences in cell invasion and wound-healing assays (Figure 3), but in attachment to various substrates, including collagen-I, the phenotype was more pronounced with QL α 12 expression. Likewise, focal adhesions were reduced, but still present with G α 12 expression (Figure 2), and the dephosphorylation of FAK and paxillin was less obvious in the G α 12-expressing cells (Figure 7). Whether the G α 12- and QL α 12-MDCK cells have an identical phenotype or a graded one may depend on the behavior being studied. Migration through a filter or in closing a wound requires numerous coordinated cellular responses, and it was in these experiments that both G α 12 and QL α 12 cells were indistinguishable. In contrast, attachment to a specific substrate is a short-term event utilizing a less complex mechanism, and in these experiments the G α 12-expressing cells often had an intermediate phenotype. This likely reflects engagement of cellular effectors under some, but not all, experimental conditions when G α 12 levels are increased. Thrombin activation of endogenous G α 12 supports several of these phenotypes, and the findings are further strengthened by the results in G α 12-silenced cells. Taken together, these cell lines consistently demonstrate G α 12 regulation of α 2 β 1 integrins on collagen-I and support the role of Rho, Src, and a tyrosine phosphatase in regulating the focal adhesion complex.

To our knowledge, this is the first report of G protein regulation of integrins in epithelial cells. We identified specific regulation of MDCK cell interactions on collagen-I (not collagen-IV) that were G α 12 regulated. This suggests important specificity in G protein regulation of integrins, although we also found G α 12-dependent attachment to laminin-1 and -5 (Figure 1 and Supplemental Figure S1). These findings raise the possibility that G α 12 may also regulate other integrins such as α 6 β 1 for laminin-1 and α 6 β 4 or α 3 β 1 for laminin-5. These findings are likely to be important in numerous contexts including epithelial migration during development and after injury, where the unique composition of the extracellular matrix will determine engagement of specific integrins. Additional studies will be necessary to explore these other mechanisms. In other cell types, there are well-characterized examples of G protein regulation of integrin function. In leukocytes, chemokine stimulated G protein-coupled receptors play a major role in regulating integrin activity and lymphocyte migration. In splenic B cells, lysophosphatidic acid regulated integrin-mediated adhesion through G α i and G α 12/13 pathways (Rieken *et al.*, 2006). In platelets, integrin-mediated aggregation can be stimulated with thrombin, ADP, epinephrine, thromboxane, and other agonists that utilize numerous G protein-coupled pathways. Costimulation of G α 12/13 and G α i pathways (with thromboxane A₂ and ADP) led to irreversible integrin (α IIb β 3)-mediated aggregation (Dorsam *et al.*, 2002; Nieswandt *et al.*, 2002).

Attachment and adhesion are critical steps in cell migration and G proteins are important in cell migration in several

different cell types. In human 1321N1 astrocytoma cells, the P2Y₂ nucleotide receptor interacts with α V integrins to induce chemotaxis. P2Y₂R also requires α V integrin to activate G α 12 and Rho pathways required for cytoskeletal rearrangements leading to chemotaxis (Liao *et al.*, 2007). In migrating leukocytes, the leading edge is dependent on G α i-mediated production of 3'-phosphoinositol lipids and activated Rac. The trailing edge uses G α 12/13 regulation of Rho, and both systems coordinate differential regulation of the actin cytoskeleton in the presence of a chemoattractant (Xu *et al.*, 2003). Using mouse embryonic fibroblast-derived G α 12/13 knockout mice, Goulimari showed that G α 12/13 were required for directed cell migration. Cells lacking G α 12/13 were unable to localize active Rho or its effector mDia at the wound edge (Goulimari *et al.*, 2005). G α 12/13-deficient fibroblasts were severely impaired in closing the gap in wound-healing assays, and the cells on the leading edge were unable to migrate in to the wounded area. On the basis of these observations, one might expect that activating G α 12 would lead to more rapid wound closure, not the inhibition that was observed in invasion and wound assays. However, there are several potential explanations for why both knockout cells and cells with an activated G α 12 might reveal a phenotype of impaired migration. First, it is likely that defects in any one of numerous critical cellular processes can result in failed migration. There are also likely to be important differences between fibroblasts and epithelial cells in the mechanisms utilized for directional migration and establishment of polarity. The defect we observe with G α 12 activation in MDCK cells is disruption of the focal adhesion protein complex and impaired lamellipodia formation. In contrast, the G α 12/13 knockout fibroblasts are lacking both G α 12 and G α 13 subunits, and these cells have impaired directional migration without any disruption of cellular process formation. MDCK cells with activated G α 12 appeared to have very few cellular processes at all.

The model suggested by our studies (Figure 9) indicates G α 12-stimulated Rho and Src leads to decreased phosphorylation of FAK and paxillin and disruption of the FAK-integrin complex. Tyrosine phosphorylation of FAK (tyr-397, -576, -577, -861, and -925) and paxillin (tyr-118) is required for assembly of the focal adhesion complex (reviewed in Mitra *et al.*, 2005). The finding of decreased tyrosine phosphorylation of these proteins with G α 12 activation is consistent with decreased migration and loss of focal adhesions. Although there was slightly decreased phosphorylation of Fak pTyr577 and paxillin pTyr118 in G α 12-expressing cells, only FAK pTyr861 was significant. Phosphorylation of FAK Tyr861 is important for assembling the protein complex necessary for cell (Kiyokawa *et al.*, 1998) migration (Kiyokawa *et al.*, 1998). Fibroblasts expressing a mutant FAK (Phe861) show decreased migration (Lim *et al.*, 2004) and in breast cancer cells, pTyr861 plays a role in transendothelial migration (Earley and Plopper, 2008). Therefore, G α 12 regulation of these phosphorylations are likely to be important to the observed phenotypes in G α 12- and QL α 12-MDCK cells. However, FAK pTyr397 and others (including pTyr861) are typically phosphorylated with Src activation, and Src can be directly activated by G α 12 (Ma *et al.*, 2000). Therefore, this traditional signaling mechanism cannot account for the decreased phosphorylation of FAK and paxillin that was observed (Figure 7, B and D). One possible explanation is that we are measuring total cellular Src activity with QL α 12 expression, and the local activity in the focal adhesion complex may be different (inhibited). Another possibility is G α 12 activation of Rho and/or Src leads to activation of a protein tyrosine phosphatase, and the

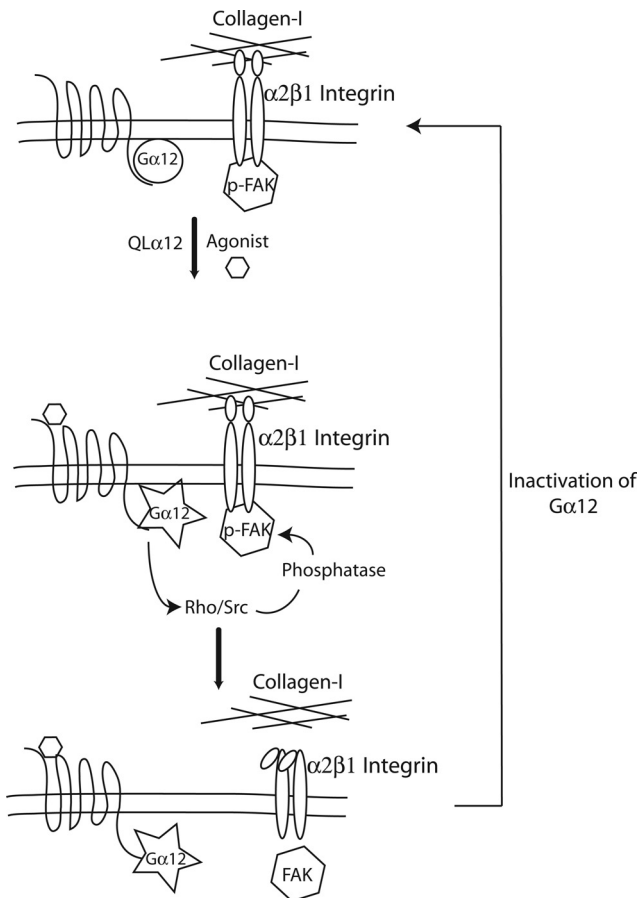


Figure 9. Model of regulation: a schematic summary of the findings in this study revealing inside-out signaling through $G\alpha_{12}$ to disrupt focal adhesions and the loss of integrin–collagen-I binding. Activation of $G\alpha_{12}$ (by thrombin or QL mutation) activates Rho and Src leading to inhibition of FAK and disruption of the FAK–integrin complex. Once the FAK–integrin complex is disrupted, the focal adhesion complex comes apart and $\alpha_2\beta_1$ integrin can no longer interact with collagen-I in the matrix. The link from Rho and Src activation to inhibition of FAK is likely mediated by intermediate signaling molecules and involves a protein tyrosine phosphatase.

results with sodium orthovanadate supports this possibility (Figure 7D). In cells overexpressing FAK, regulation of pTyr576–577 by a protein phosphatase was suggested by treatment with orthovanadate (Earley and Plopper, 2008), and sodium orthovanadate is known to be a broad inhibitor of protein tyrosine phosphatases. The mechanisms of focal adhesion complex assembly are known in some detail, yet there is little known about the phosphatases regulating focal adhesions. The nontransmembrane phosphotyrosyl phosphatase, SHP-2, is widely expressed and was shown to be required for cell migration and branching morphogenesis in MDCK cell 3D culture (Wang *et al.*, 2006). SHP-2 associates with FAK in HCA-7 cells and directly tyrosine dephosphorylated FAK in vitro (Khare *et al.*, 2006). In addition, there is evidence that Src can activate SHP-1 in embryonic tissues (Alvarez *et al.*, 2008), suggesting the possibility that Src may stimulate SHP-2 in other contexts. Another phosphatase (low-molecular-weight phosphotyrosine protein phosphatase) was shown to regulate FAK phosphorylation in a Src-dependent manner, and overexpression led to decreased cell spreading and decreased focal adhesions (Rigacci *et al.*, 2002). Additional studies will be needed to address these

potential mechanisms and identify the relevant protein tyrosine phosphatase(s).

The finding that this signaling pathway is likely to involve a protein phosphatase is consistent with several other reports linking $G\alpha_{12}$ signaling to protein phosphatases. We identified direct binding of $G\alpha_{12}$ to the scaffolding (A) subunit of the serine/threonine phosphatase PP2A and demonstrated that $G\alpha_{12}$ -stimulated phosphatase activity (Zhu *et al.*, 2004, 2007). Activated $G\alpha_{12}$ and $G\alpha_{13}$ have been shown to bind and stimulate the PP5 family of serine/threonine phosphatases (Yamaguchi *et al.*, 2002, 2003) through an interaction with the TPR (tetratricopeptide repeat) domain. These observations, in addition to the studies presented here, suggest that $G\alpha_{12/13}$ may be important regulators of cellular phosphatases. The findings in this report are the first to implicate regulation of a protein tyrosine phosphatase, and the $G\alpha_{12}$ regulation in this case is likely to be indirect.

The pathophysiologic implications for these studies extend beyond potential roles in metastatic epithelial cancers. The 3D collagen-I gel model of branching morphogenesis in MDCK cells has been widely utilized because it recapitulates many of the *in vivo* steps that are seen with the iterative branching morphogenesis of the ureteric bud. Work from many laboratories reveals a multistep process that requires cell adhesion to the extracellular matrix, cell spreading, and cell migration to form tube-like structures. In addition, there is a balance between proliferation and apoptosis required for successful tubule development (reviewed in Pohl *et al.*, 2000; O'Brien *et al.*, 2002). Integrins are essential for branching tubulogenesis in 3D collagen-I culture and the $\alpha_1\beta_1$ integrins are required along with other integrin families that utilize laminin receptors ($\alpha_3\beta_1$, $\alpha_6\beta_1$, and $\alpha_6\beta_4$ integrins) (Chen *et al.*, 2004). Our finding of impaired tubulogenesis and increased cyst-like structures reveals novel regulation of integrins through activation of $G\alpha_{12}$ and inhibition $\alpha_2\beta_1$ function in 3D collagen-I matrix. Activated Rho may also contribute to the defective tubule formation seen in QL α_{12} -MDCK cells. Loss of FAK leads to activation of Rho and inhibition of focal adhesion turnover (Ren *et al.*, 1999), and RhoA inactivation is necessary for cell spreading and migration (Arthur and Burridge, 2001). Integrins normally trigger inhibition of RhoA through Src-dependent activation of p190RhoGAP (Arthur *et al.*, 2000), and this inhibition is likely to be blocked in this model with $G\alpha_{12}$ activation.

The cysts seen in the 3D tubulogenesis assays with $G\alpha_{12}$ activation raises the possibility that $G\alpha_{12}$ could play a role in the development of cystic kidney diseases. PC1 encodes a large transmembrane protein, polycystin-1 (PC1), that is localized to cilia, adherens junctions, and the basal membrane of renal epithelia. PC1 has a short intracellular cytoplasmic domain that binds to $G\alpha_{12}$ (Yuasa *et al.*, 2004). Mutations in PC1 mutations are responsible for the majority of patients with ADPKD, and several studies have linked changes in integrin expression and function in ADPKD. Similar to what we observe with $G\alpha_{12}$ -stimulated inhibition of $\alpha_2\beta_1$ integrin function, studies with MDCK cells transfected with antisense RNA for α_2 integrins led to reduced adhesion to collagen-I, decreased tubulogenesis, and the formation of cyst-like structures in 3D (Saelman *et al.*, 1995). In MDCK cells with silenced PC1 expression, tubulogenesis was inhibited and there was increased adhesion to collagen-I associated with up-regulation of $\alpha_2\beta_1$ integrin protein level (Battini *et al.*, 2006). In addition to MDCK cell models, there is also evidence for a PC1- α_2 -integrin link. In human immortalized renal epithelial cell lines derived from normal kidney and ADPKD kidneys, ADPKD renal cells showed increased adhesion to collagen-I and showed increased lev-

els of α 2 β 1 integrin expression when compared with controls. Confocal microscopy revealed colocalization of α 2 β 1 integrins and PC1 along with vinculin in focal adhesions (Wilson *et al.*, 1999). Furthermore, the impaired cell migration observed in QL α 12-MDCK cells, and the increased Rho activity may contribute to cyst development. In support of this possibility, we find that inhibiting Rho in *Pkd1* mutant mouse embryonic kidney cells (*Pkd1*^{-/-}) growing in 3D collagen-I culture leads to a reversal of the cystic phenotype and the development of a branching morphology. This suggests that G α 12/Rho activation may be required for the maintenance of cystogenesis (unpublished data). These findings, taken together, lead us to speculate that there is important regulation of epithelial cell functions through PC1/G α 12.

In conclusion, we find that G α 12 inhibits α 2 β 1 integrins in epithelial cells and leads to defects in cell spreading that impairs cell migration and prevents tubulogenesis in 3D culture. These findings provide novel insights into epithelial cell functions that are likely to be important in several areas of epithelial pathobiology and include metastasis, tubulogenesis during renal development, recovery from acute kidney injury and in the pathogenesis of polycystic kidney disease. Strategies to block G α 12 signaling may hold promise for treating the adverse consequences seen in these disorders.

ACKNOWLEDGMENTS

We thank members of the Harvard Polycystic Kidney Disease Center for helpful comments and suggestions, Dr. Gunaratnam for providing G α 12-expressing PK1 cells, and Sarah Beaudry for her outstanding technical assistance. This work was supported by Grants P50 DK074030 to J.Z. (PI) and B.M.D. (Project 1). J.Z. is also supported by R01 KD40703 and B.M.D. by R01 GM5223, and Grant K01 DK080179 to T.K.

REFERENCES

- Alvarez, S. E., Seguin, L. R., Villarreal, R. S., Nahmias, C., and Ciuffo, G. M. (2008). Involvement of c-Src tyrosine kinase in SHP-1 phosphatase activation by Ang II AT2 receptors in rat fetal tissues. *J. Cell. Biochem.* 105, 703–711.
- Arthur, W. T., and Burridge, K. (2001). RhoA inactivation by p190RhoGAP regulates cell spreading and migration by promoting membrane protrusion and polarity. *Mol. Biol. Cell* 12, 2711–2720.
- Arthur, W. T., Petch, L. A., and Burridge, K. (2000). Integrin engagement suppresses RhoA activity via a c-Src-dependent mechanism. *Curr. Biol.* 10, 719–722.
- Battini, L., Fedorova, E., Macip, S., Li, X., Wilson, P. D., and Gusella, G. L. (2006). Stable knockdown of polycystin-1 confers integrin- α 2 β 1-mediated anoikis resistance. *J. Am. Soc. Nephrol.* 17, 3049–3058.
- Boca, M., D'Amato, L., Distefano, G., Polishchuk, R. S., Germino, G. G., and Boletta, A. (2007). Polycystin-1 induces cell migration by regulating phosphatidylinositol 3-kinase-dependent cytoskeletal rearrangements and GSK3 β -dependent cell cell mechanical adhesion. *Mol. Biol. Cell* 18, 4050–4061.
- Buhl, A. M., Johnson, N. L., Dhanasekaran, N., and Johnson, G. L. (1995). G α 12 and G α 13 stimulate Rho-dependent stress fiber formation and focal adhesion assembly. *J. Biol. Chem.* 270, 24631–24634.
- Chen, D., *et al.* (2004). Differential expression of collagen- and laminin-binding integrins mediates ureteric bud and inner medullary collecting duct cell tubulogenesis. *Am. J. Physiol. Renal. Physiol.* 287, F602–F611.
- Dorsam, R. T., Kim, S., Jin, J., and Kunapuli, S. P. (2002). Coordinated signaling through both G12/13 and G(i) pathways is sufficient to activate GPIIb/IIIa in human platelets. *J. Biol. Chem.* 277, 47588–47595.
- Earley, S., and Plopper, G. E. (2008). Phosphorylation of focal adhesion kinase promotes extravasation of breast cancer cells. *Biochem. Biophys. Res. Commun.* 366, 476–482.
- Goulimari, P., Kitzing, T. M., Knieling, H., Brandt, D. T., Offermanns, S., and Grosse, R. (2005). G α 12/13 is essential for directed cell migration and localized Rho-Dia1 function. *J. Biol. Chem.* 280, 42242–42251.
- Hynes, R. O. (2002). Integrins: bidirectional, allosteric signaling machines. *Cell* 110, 673–687.
- Joly, D., Morel, V., Hummel, A., Ruello, A., Nusbaum, P., Patey, N., Noel, L. H., Rousselle, P., and Knebelmann, B. (2003). β 4 integrin and laminin 5 are aberrantly expressed in polycystic kidney disease: role in increased cell adhesion and migration. *Am. J. Pathol.* 163, 1791–1800.
- Kelly, P., Casey, P. J., and Meigs, T. E. (2007). Biologic functions of the G12 subfamily of heterotrimeric G proteins: growth, migration, and metastasis. *Biochemistry* 46, 6677–6687.
- Kelly, P., Moeller, B. J., Juneja, J., Booden, M. A., Der, C. J., Daaka, Y., Dewhirst, M. W., Fields, T. A., and Casey, P. J. (2006a). The G12 family of heterotrimeric G proteins promotes breast cancer invasion and metastasis. *Proc. Natl. Acad. Sci. USA* 103, 8173–8178.
- Kelly, P., Stemmler, L. N., Madden, J. F., Fields, T. A., Daaka, Y., and Casey, P. J. (2006b). A role for the G12 family of heterotrimeric G proteins in prostate cancer invasion. *J. Biol. Chem.* 281, 26483–26490.
- Khare, S., Holgren, C., and Samarel, A. M. (2006). Deoxycholic acid differentially regulates focal adhesion kinase phosphorylation: role of tyrosine phosphatase Shp2. *Am. J. Physiol. Gastrointest. Liver Physiol.* 291, G1100–G1112.
- Kiyokawa, E., Hashimoto, Y., Kobayashi, S., Sugimura, H., Kurata, T., and Matsuda, M. (1998). Activation of Rac1 by a Crk SH3-binding protein, DOCK180. *Genes Dev.* 12, 3331–3336.
- Kolesnikova, T. V., Mannion, B. A., Berditchevski, F., and Hemler, M. E. (2001). β 1 integrins show specific association with CD98 protein in low density membranes. *BMC Biochem.* 2, 10.
- Kozasa, T., Jiang, X., Hart, M. J., Sternweis, P. M., Singer, W. D., Gilman, A. G., Bollag, G., and Sternweis, P. C. (1998). p115 RhoGEF, a GTPase activating protein for G α 12 and G α 13. *Science* 280, 2109–2111.
- Liao, Z., Seye, C. L., Weisman, G. A., and Erb, L. (2007). The P2Y2 nucleotide receptor requires interaction with α v integrins to access and activate G12. *J. Cell Sci.* 120, 1654–1662.
- Lim, Y., Han, I., Jeon, J., Park, H., Bahk, Y. Y., and Oh, E. S. (2004). Phosphorylation of focal adhesion kinase at tyrosine 861 is crucial for Ras transformation of fibroblasts. *J. Biol. Chem.* 279, 29060–29065.
- Ma, Y. C., Huang, J., Ali, S., Lowry, W., and Huang, X. Y. (2000). Src tyrosine kinase is a novel direct effector of G proteins. *Cell* 102, 635–646.
- Meigs, T. E., Fedor-Chaikin, M., Kaplan, D. D., Brackenbury, R., and Casey, P. J. (2002). G α 12 and G α 13 negatively regulate the adhesive functions of cadherin. *J. Biol. Chem.* 277, 24594–24600.
- Meyer, T. N., Hunt, J., Schwesinger, C., and Denker, B. M. (2003). G α 12 regulates epithelial cell junctions through Src tyrosine kinases. *Am. J. Physiol. Cell Physiol.* 285, C1281–C1293.
- Meyer, T. N., Schwesinger, C., and Denker, B. M. (2002). Zonula occludens-1 is a scaffolding protein for signaling molecules. G α 12 directly binds to the Src homology 3 domain and regulates paracellular permeability in epithelial cells. *J. Biol. Chem.* 277, 24855–24858.
- Mitra, S. K., Hanson, D. A., and Schlaepfer, D. D. (2005). Focal adhesion kinase: in command and control of cell motility. *Nat. Rev. Mol. Cell Biol.* 6, 56–68.
- Nieswandt, B., Schulte, V., Zywietz, A., Gratacap, M. P., and Offermanns, S. (2002). Costimulation of Gi- and G12/G13-mediated signaling pathways induces integrin α IIb β 3 activation in platelets. *J. Biol. Chem.* 277, 39493–39498.
- O'Brien, L. E., Zegers, M. M., and Mostov, K. E. (2002). Opinion: Building epithelial architecture: insights from three-dimensional culture models. *Nat. Rev. Mol. Cell Biol.* 3, 531–537.
- Pohl, M., Stuart, R. O., Sakurai, H., and Nigam, S. K. (2000). Branching morphogenesis during kidney development. *Annu. Rev. Physiol.* 62, 595–620.
- Pollack, A. L., Runyan, R. B., and Mostov, K. E. (1998). Morphogenetic mechanisms of epithelial tubulogenesis: MDCK cell polarity is transiently rearranged without loss of cell-cell contact during scatter factor/hepatocyte growth factor-induced tubulogenesis. *Dev. Biol.* 204, 64–79.
- Ren, X. D., Kiosses, W. B., and Schwartz, M. A. (1999). Regulation of the small GTP-binding protein Rho by cell adhesion and the cytoskeleton. *EMBO J.* 18, 578–585.
- Rieken, S., Herroeder, S., Sassmann, A., Wallenwein, B., Moers, A., Offermanns, S., and Wettschreck, N. (2006). Lysophospholipids control integrin-dependent adhesion in splenic B cells through G(i) and G(12)/G(13) family G-proteins but not through G(q)/G(11). *J. Biol. Chem.* 281, 36985–36992.
- Rigacci, S., Rovida, E., Dello Sbarba, P., and Berti, A. (2002). Low Mr phosphotyrosine protein phosphatase associates and dephosphorylates p125 focal adhesion kinase, interfering with cell motility and spreading. *J. Biol. Chem.* 277, 41631–41636.

- Riobo, N. A., and Manning, D. R. (2005). Receptors coupled to heterotrimeric G proteins of the G12 family. *Trends Pharmacol. Sci.* 26, 146–154.
- Sabath, E., Negoro, H., Beaudry, S., Paniagua, M., Angelow, S., Shah, J., Grammatikakis, N., Yu, A. S., and Denker, B. M. (2008). $G\alpha_{12}$ regulates protein interactions within the MDCK cell tight junction and inhibits tight-junction assembly. *J. Cell Sci.* 121, 814–824.
- Saelman, E. U., Keely, P. J., and Santoro, S. A. (1995). Loss of MDCK cell $\alpha_2\beta_1$ integrin expression results in reduced cyst formation, failure of hepatocyte growth factor/scatter factor-induced branching morphogenesis, and increased apoptosis. *J. Cell Sci.* 108(Pt 11), 3531–3540.
- Wang, C. Z., Su, H. W., Hsu, Y. C., Shen, M. R., and Tang, M. J. (2006). A discoidin domain receptor 1/SHP-2 signaling complex inhibits $\alpha_2\beta_1$ -integrin-mediated signal transducers and activators of transcription 1/3 activation and cell migration. *Mol. Biol. Cell* 17, 2839–2852.
- Wang, X. Q., and Frazier, W. A. (1998). The thrombospondin receptor CD47 (IAP) modulates and associates with $\alpha_2\beta_1$ integrin in vascular smooth muscle cells. *Mol. Biol. Cell* 9, 865–874.
- Wilson, P. D., Geng, L., Li, X., and Burrow, C. R. (1999). The PKD1 gene product, “polycystin-1,” is a tyrosine-phosphorylated protein that colocalizes with $\alpha_2\beta_1$ -integrin in focal clusters in adherent renal epithelia. *Lab. Invest.* 79, 1311–1323.
- Xu, J., *et al.* (2003). Divergent signals and cytoskeletal assemblies regulate self-organizing polarity in neutrophils. *Cell* 114, 201–214.
- Yamaguchi, Y., Katoh, H., Mori, K., and Negishi, M. (2002). $G\alpha_{12}$ and $G\alpha_{13}$ interact with Ser/Thr protein phosphatase type 5 and stimulate its phosphatase activity. *Curr. Biol.* 12, 1353–1358.
- Yamaguchi, Y., Katoh, H., and Negishi, M. (2003). N-terminal short sequences of α subunits of the G12 family determine selective coupling to receptors. *J. Biol. Chem.* 278, 14936–14939.
- Yanamadala, V., Negoro, H., Gunaratnam, L., Kong, T., and Denker, B. M. (2007). $G\alpha_{12}$ stimulates apoptosis in epithelial cells through JNK1-mediated Bcl-2 degradation and up-regulation of I κ B α . *J. Biol. Chem.* 282, 24352–24363.
- Yang, X. H., Richardson, A. L., Torres-Arzayus, M. I., Zhou, P., Sharma, C., Kazarov, A. R., Andzelm, M. M., Strominger, J. L., Brown, M., and Hemler, M. E. (2008). CD151 accelerates breast cancer by regulating α_6 integrin function, signaling, and molecular organization. *Cancer Res.* 68, 3204–3213.
- Yuasa, T., Takakura, A., Denker, B. M., Venugopal, B., and Zhou, J. (2004). Polycystin-1L2 is a novel G-protein-binding protein. *Genomics* 84, 126–138.
- Zhu, D., Kosik, K. S., Meigs, T. E., Yanamadala, V., and Denker, B. M. (2004). $G\alpha_{12}$ directly interacts with PP2A: evidence for $G\alpha_{12}$ -stimulated PP2A phosphatase activity and dephosphorylation of microtubule-associated protein, tau. *J. Biol. Chem.* 279, 54983–54986.
- Zhu, D., Tate, R. I., Ruediger, R., Meigs, T. E., and Denker, B. M. (2007). Domains necessary for $G\alpha_{12}$ binding and stimulation of protein phosphatase-2A (PP2A): is $G\alpha_{12}$ a novel regulatory subunit of PP2A? *Mol. Pharmacol.* 71, 1268–1276.
- Zylstra, S., Chen, F. A., Ghosh, S. K., Repasky, E. A., Rao, U., Takita, H., and Bankert, R. B. (1986). Membrane-associated glycoprotein (gp 160) identified on human lung tumors by a monoclonal antibody. *Cancer Res.* 46, 6446–6451.